CHAPTER 2

LITERATURE REVIEW

2.1 INTRODUCTION

WELDING, the fusing of the surfaces of two work pieces to form one is a precise, reliable, cost-effective, and "high-tech" method for joining materials. No other technique is as widely used as welding, by manufacturers to join metals and alloys efficiently and to add value to their products. Most of the familiar objects in modern society, from buildings and bridges, to vehicles, computers, and medical devices, could not be produced without the use of welding.

In fusion welding, weld profile imperfections like lack of penetration, lack of fusion and undercut are resulted may be because of welding parameters selected incorrectly or poor welder technique. Aluminium has high thermal conductivity and solidification of weld pool is faster hence it is susceptible to profile imperfections [17].

Friction Stir Welding is proved to be cost effective, sustainable, energy-efficient and environment friendly process in 21st century. It has bright future in fabrication industries because it is adding the value and reducing defects compare to fusion welding. It has the specialty of joining dissimilar metals and alloys which have totally different compositions and also can weld non-metallic materials.

The 1996 Occupational Outlook Handbook [18] published by the U.S. Bureau of Labor Statistics indicates that over 450,000 Americans were employed as welders, cutters, and welding machine operators. By including the workers from these professions that are directly involved in welding, the size of the welding community swells to over 2 million workers, or over 10 percent of the manufacturing workforce. This indicates the future demand and scope of development in the field of welding.

2.2   CONVENTIONAL FRICTION STIR WELDING (CFSW)

In FSW process, a cylindrical rotating tool is plunged into the abutting edges of the work-pieces to be joined, whereby the shoulder has intimate contact with the top surface of the material while the pin is fully penetrated into the material, as shown in Figure 2.1. The heating and stirring of material by the tool from the advancing side (AS) to the retreating side (RS) while traversing through the material, creating a joint line at the trailing of the tool (Figure 2.1(a)). The temperature of the material is raised upto 80% of the melting point due to very high shearing force involved in the process. The plates to be joined require strong and rigid clamping both in the vertical and horizontal directions to prevent them being separated by the high forces exerted by the CFSW tool. In addition, a rigidly supported plate (also known as backing plate or anvil) is used to counteract the vertical force, see Figure 2.1(b). In short, zero degrees of freedom are expected to achieve quality welds. Also the backing plate should be free from oil or any type of contaminant; otherwise it will be trapped into the weld. This arrangement slows setup time and limits the thickness of parts that can be welded by this process.

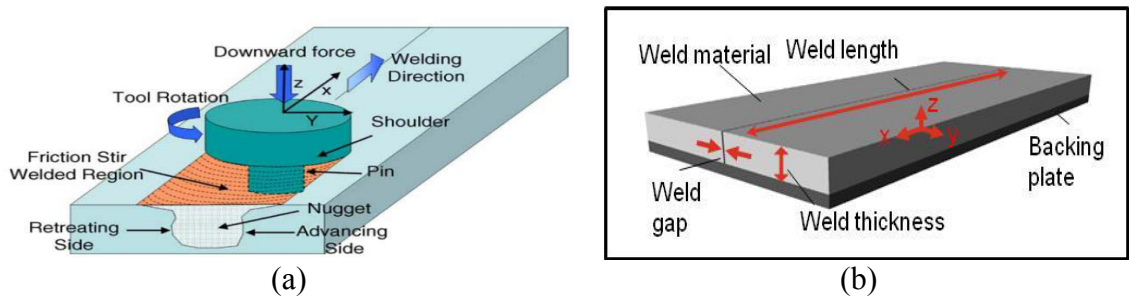(a)   (b)

Figure 2.1: FSW setup (a) The illustration of FSW process [8], (b) Schematic Diagram of Material Constraints [19].

The Z axis is taken as perpendicular to the substrate surface, X is in the direction of the weld progression, and Y is transverse to the weld line, as in the figure above.

2.2.1 Process steps

As illustrated in Figure 2.2, there are four basic steps - tool rotation, tool plunge, tool traverse and tool withdrawal. To provide sufficient heat for welding, dwell phase is added before starting tool traversing and after completion of weld (before tool unplunging).
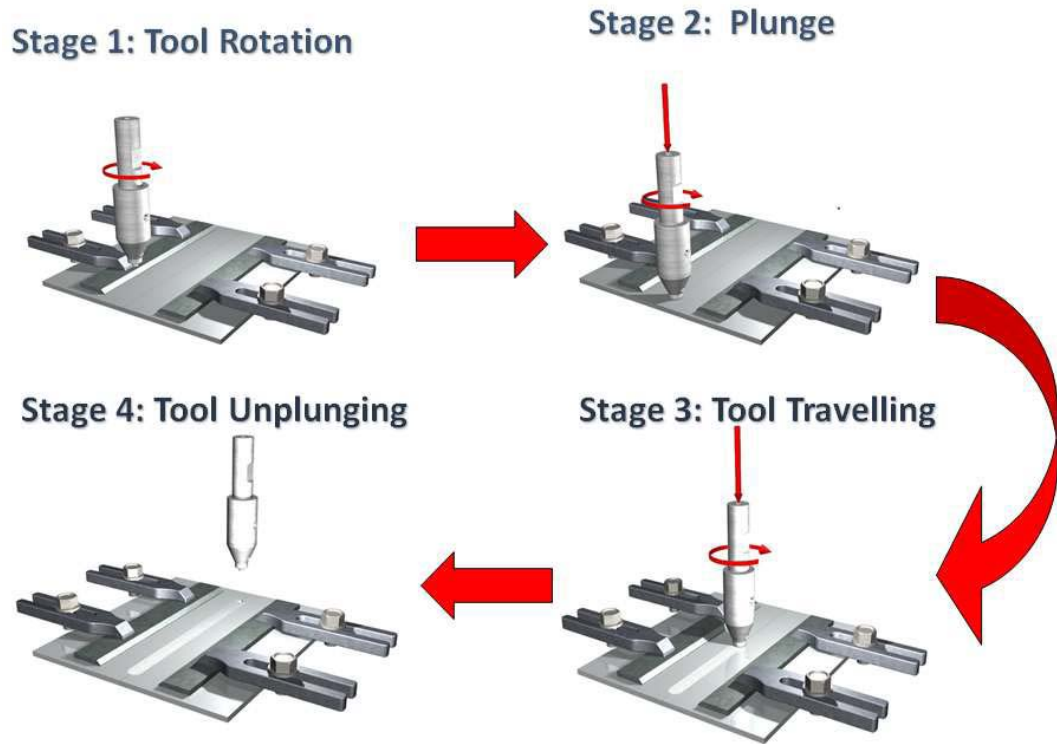
Figure 2.2: FSW process steps [20]

2.2.1.1   Tool Plunge

Plunging of tool in work substrate is very important phase. There are chances of tool failure either from unheated or prewelded material. The quality of weld depends upon depth of tool or tool penetration. Higher penetration will break the tool or would cause the defect, while incomplete penetration will result in poor bonding [21]. Position or force control or a combination of both can be used to regulate the plunge depth.

2.2.1.2   Tool Traverse

This stage of the operation creates the joint between the pre-welded sections of material. Once the tool is plunged to the proper depth and sufficient heat is produced by tool, the feed table or tool traverse is initiated. As the tool is pulled through the heated and plasticized material, the material flows around the contours of the tool towards the rear of the tool where it cools to form the joint.

2.2.1.3   Unplunging or Run Off

The tool is withdrawn from the material after welding is completed. An exit hole (dimple) is left by the tool profile in CFSW and run out in BFSW as shown in Figure 2.3. For this reason a run off area is required at the end of the weld in case of CFSW and at both the ends in case of BFSW; which is usually trimmed off after the process. A retracting probe is an advancement which solves this problem in CFSW [22].
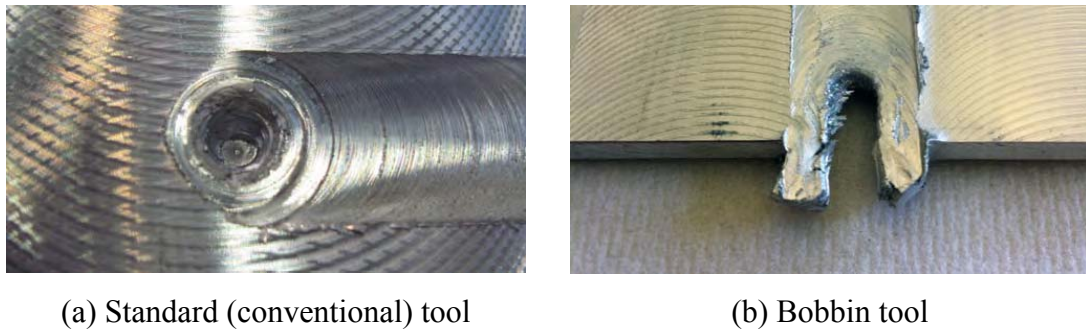

(a) Standard (conventional) tool   (b) Bobbin tool

Figure 2.3: Typical exit holes and run-outs produced when the Tool is removed from the Material

2.2.2 Bobbin Friction Stir Welding (BFSW)

The bobbin friction stir welding (BFSW) tool has two shoulders with one on the top surface and the other on the bottom surface of the weld plate, with a pin fully contained inside the material. This reduces the requirements of extensive clamping and setup prior to welding. The vertical down force imposed by standard FSW is reduced in this case and reactive forces withic the weld are contained between the bobbin (two) shoulders. There are three types of bobbin tool; fixed bobbin, floating bobbin and adaptive bobbin [23][24]. The definitions of these variants are explained as follows:

- Fixed bobbin - The gaps are fixed between the two shoulders throughout the process and the normal Z-axis movement of the tool can be either fixed or controlled based on system capability (Figure 2.4 (a)).

- Floating bobbin - The two shoulders have a fixed gap throughout the process and thus produce balanced forces in the Z-axis (Figure 2.4 (b)). However, the tool floats in the Z direction throughout the process.

- Adaptive bobbin (AdAPT): The adaptive technique enables adjustment of the gap between the shoulders during the welding operation while the tool floats in the Z direction [Figure 2.4 (c)].
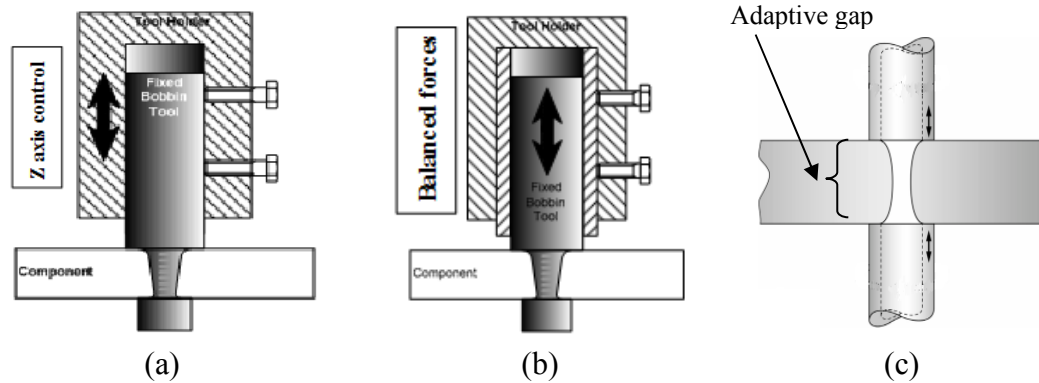

Figure 2.4: Bobbin Tools. (a) Fixed gap [23], (b) Floating [23], (c) AdAPT [24]

When floating or adaptive bobbin tools are used, the Z forces should be near to zero. In addition to the above tool configurations, there are also discussions by TWI about the development of double driven bobbin (top shoulder and bottom shoulder driven) which can also include an adjustable shoulder gap. These developments along with many others are closely guarded due to the intellectual property (IP) potential.

According to the TWI [23], the industrial uptake of bobbin tool FSW has been limited by a perception that the equipment required to implement is complex and expensive. This includes concern on ease of the technology implementation. However, the most basic configuration of bobbin tool application can be implemented on most of the currently available CFSW facilities; especially the fixed bobbin format.

2.2.3 Comparison between CFSW and BFSW

High clamping forces and proper setup prior to welding is essential for CFSW. Improper process setup results into defects like incomplete weld penetration, backing plate contamination and voids. Furthermore, when lower temperatures are produced during the process, the material flow from the advancing to the retreating tool edge cannot always

be completed, hence defects such asvoids, tunnel and kissing bonds are produced [7].

Normally high tool rotational speed and lower tool traversing speeds are required to maintain sufficient welding temperature in CFSW, but it may not be true assumption in case of BFSW. The conventional FSW tools typically run at a travel speed of 150 mm/min and spindle speed reached 1000 rpm [8]. While, for BFSW 300 mm/min and 300 rpm rotational speed for welding AA6082-T6 Aluminium Alloy was used [13].

With the introduction of bobbin tooling, welding setup and weld defects are found to be minimized or eliminated. It is because of the reduced clamping force and generation of sufficient heat for stirring and mixing of material in the weld region. The additional advantages of the BFSW process are listed. This is based on the understanding that obtained from both processes through literatures, example in [7][12][25][26].

Advantages of BFSW:
a) Ease of clamping.
b) Incomplete/partial root penetration is negligible.
c) Spindle rotational speeds lower than CFSW.
d) Allows higher welding speed (tool traverse speed) as compare to CFSW, due to the heating from both shoulders.
e) Backing bar/plate not required.

2.2.4 FSW Process variables

Mechanical engagement of FSW tool with substrate generates heat and pressure. These cause materials atoms of adjacent surfaces to come into close proximity to form joint. The oxide and contamination layer that are present on the plates are disrupted during the process. The degree of heat and pressure are affected by many variables. Based on previous studies for CFSW, if the welding objective is to obtain defect free welds, some factors that should be taken into account are axial force, rotation speed, traverse speed, tool tilt angle and tool geometry [7]. More generally, Mishra and Ma [8] stated that the major factors affecting the FSW process are tool geometry, joint design and process variables such as tool rotation and traverse speed. Regardless of the type of FSW process

(CFSW or BFSW), factors that affect the weld output quality and consistency are shown in Figure 2.5, a cause and effect diagram by Lakshminarayanan and Balasubramanian [27].

As stated earlier, two main elements for joint formation in FSW are heat and pressure. But weld quality also requires good material flow, which arises from the motion [28]. The dominant process parameters (inputs) which are commonly stated by previous researchers are spindle speed, travel speed and tool design [13][29][30][31][32][33].
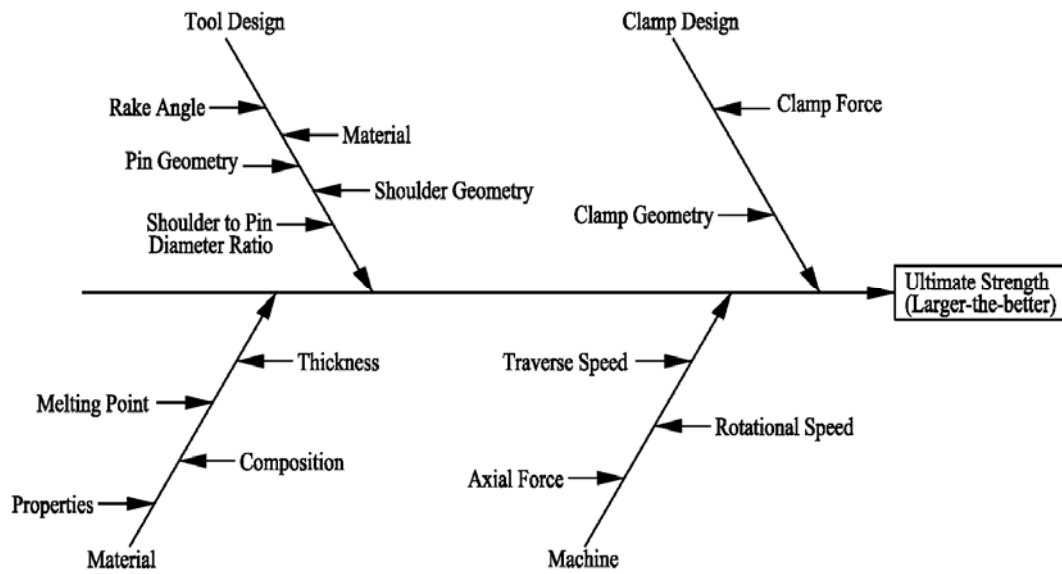

Figure 2.5: Cause and effect diagram for FSW process [27]

As shown in Figure 2.6, a range of feed ratio *(k)* can be determined either experimentally [34] or numerically to obtain an acceptable weld quality under given welding conditions (material type, material thickness, tool shape).

$$k = v / \omega \tag{2.1}$$

Where: (k) feed ratio (mm/rev),

(v) Welding speed (mm/s),
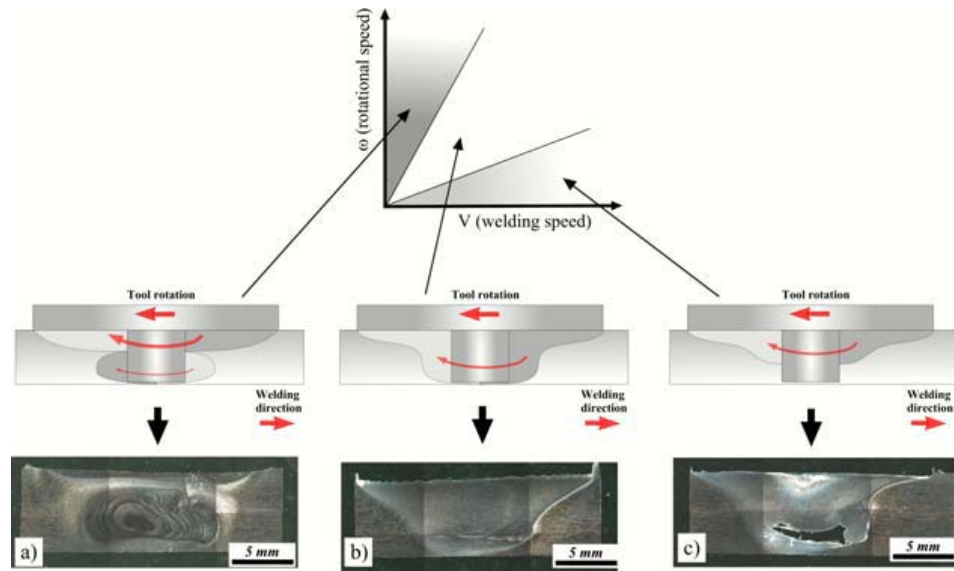
(ω) Rotational speed (rev/s).

Figure 2.6: Weld quality as function of feed ratio. FSW of AA6061, thickness of 8 mm [34]

If tool rotational speed is high and traversing speed is low then it will result into hot weld. An over stirred condition may occur as shown in figure 2.6(a). The material in this zone may be spinned more than in the weld bottom, resulting in to double nuggets or wormhole defect. If tool rotational speed is lower and traversing speed is high then it will result in to cold welding, (figure 2.6(c)) in which case stable material flow may not be established causing lack of material feeding at bottom having tunnel type defect. An optimization between these two conditions is required to have stable boundary layer and defect free sound weld as shown in Figure 2.6(b).

2.3   FSW TOOLING

The major considerations covered under the tooling for FS welding are clamp design, tool design and machine tool used. Out of this, a machine tool has choice limited to selection rather than design. Either you can use the machine tool available or hire or procure, looking to the specifications suitable to torque requirement. Proper clamping of the substrate is essential which will restrict linear and transverse movements. Also the vertical lifting in Z-direction should be arrested. Tool design covers tool features, tool dimensions and tool material.

2.3.1 Clamping of substrate

Proper clamping of plates to be joined is very important and difficult task in friction stir welding process. The substrates must be clamped on strong and rigid backing plate during welding. The vertical and forces tend to lift and push the work apart respectively. The clamping system should be such that it will restrain the work and keep them from moving apart. A root opening gap is acceptable upto 10% of the thickness of work material less than 13mm. The top clamping should kept closer to the tool i.e. close to the joint which will reduce thee clamping load.

As stated above, proper clamping of substrate is a basic need in CFSW, as defects can be observed due to improper setup. Also in case of BFSW clamping forces are reduced due to double shoulder developing sufficient heat for stirring. But it doesn't mean that the clamping is not essential. A typical clamp design is expected in BFSW which is not at all of less importance than in CFSW.

Looking to the above requirements, it is observed that different methods are adopted to clamp the work-piece. People have tried to fulfill the requirements, but hardly any literature is available giving complete understanding of fixture design. Prashant Prakash et al. [35] used the simplest way of clamping as shown in Figure 2.7.

Figure 2.7: Setting the Al plates in Universal Milling Machine [35]

In majority of the cases workshop equipment [36][37][38][39] are used to hold substrate in position (Figure 2.8).
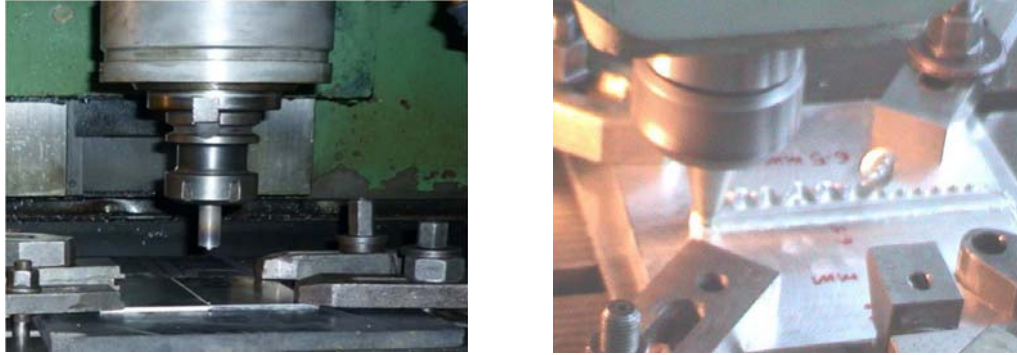
Figure 2.8: Clamping of plates using workshop clamps [36][37]

Navdeep Singh et al. [40] adopted a welding technique in fabrication of fixture (Figure 2.9). There are chances of distortion of fixture itself which will affect the accuracy of clamping and hence the quality of welding.

Figure 2.9: Fabrication of fixture using welding technique [40]

P. Prasanna et al. [41] tried to fulfill the requirement for clamping the substrate by arresting horizontal and vertical movement shown in Figure 2.10.
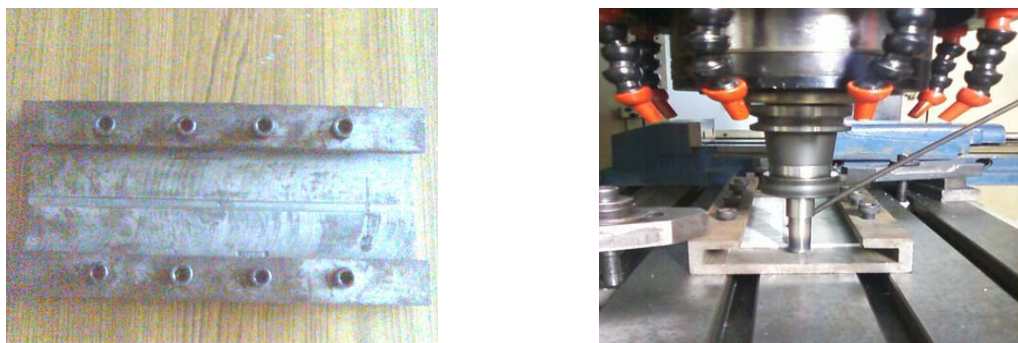

Figure 2.10: Fixture with horizontal movement restricted in X-direction and vertical clamping at edge [41]

2.3.2 Tool Design

Principally there are three functions of tool in FSW process (i) generate heat, (ii) to plasticize the material and (iii) displace material to create uniform welded joint. Consequently to ensure weld quality the proper tool design and selection of process parameters are essential [42].

As illustrated in Figure 2.11, the FSW tools have two major primary features; the shoulder and pin (also known as probe). Minton [19] has classified a range of additional secondary features known as external features on the tool e.g. threads and tapers. In his work, Minton grouped all of these external features into one and referred to them as a tertiary features but in this thesis the author will refer to them as secondary features. Examples of secondary features are shown in Figure 2.11 threaded tapered pin with a concave shoulder and Figure 2.11 threaded, tapered pin with three flutes and scrolled shoulder.

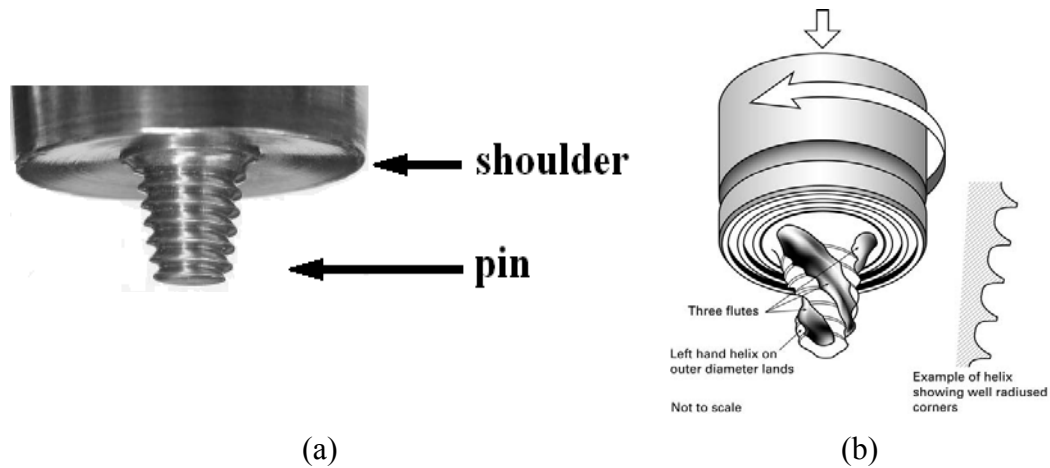(a)   (b)

Figure 2.11: FSW tool for CFSW [12] (a) Threaded tapered pin with a concave shoulder
(b) Threaded, tapered with three flutes pin and scrolled shoulder [43].

2.3.2.1   Tool Material

Friction stirring is a thermo mechanical deformation process where the tool temperature approaches the solidus temperature of base metal. To achieve weld quality in friction stir welds, along with tool design a tool material selection is also equally important. The tool material should be such that it can withstand temperature developed during welding

through friction. The tool material should be stronger and wear resistant and should have higher melting point than work material. Aluminium can be joined using a tool made from tool steel [44].

To weld steel, the tool material should be more temperature resistant i.e. tungsten or tungsten carbide. This means the selection of an FSW tool material must be based on the weld material properties. There are other type of tool material under investigation like ceramic. A ceramic tool is more resistant to abrasion and so will not wear as much. This tool would also be able to generate the temperatures required to join steels. Ceramic although tough is a more brittle substance than metal and so the traversing of the tool would be its biggest challenge.

Table 2.1 shows the most commonly used tool materials for different base materials and thicknesses:

Table 2.1: Summary of tool materials for friction stir welding [12]

Alloys to be welded	Thickness (mm)	Tool material
Aluminium alloys	<50	Tool steel, WC-Co
Copper and Copper alloys	<50	Ni alloys, W alloys, PCBN, tool steel
Magnesium alloys	<06	Tool steel, WC
Titanium alloys	<06	Tungsten alloys
Stainless steels	<06	PCBN, Tungsten alloys
Low-alloy steels	<10	WC, PCBN
Nickel alloys	<06	PCBN

The following characteristics have to be considered for proper tool material selection:
- Ambient and high temperature strength,
- Elevated temperature stability
- Wear resistance,

- Tool reactivity,

- Fracture toughness,

- Coefficient of thermal expansion,

- Machinability,

- Availability of materials.

➢ Hot work tool steels: it is the most common tool material having advantageous characteristics like easy availability, machinability, thermal fatigue resistance; wear resistance, low cost, etc. AISI H13 is chromium- molybdenum hot worked air hardened steel suitable for aluminium and thin copper sheets.

➢ Nickel and Cobalt base Alloys: it has high strength, excellent ductility, creep resistance, hardness stability and corrosion resistance. These alloys derive their strength from precipitates, so the operational temperature range must be kept below the precipitation temperature (typically 600 to 800º C).

➢ Refractory metals: tungsten, molybdenum and tantalum are having high temperature strength. They are the strongest alloys between 1000-1500 C, expensive, difficult to machine, and brittle because of powder processing technique generally adopted in production of these tools.

➢ Carbide particles metal matrix composites (WC, WC-Co, TiC): it has superior wear resistance, high temperature strength and reasonable fracture toughness.

➢ Polycrystalline cubic boron nitride (PCBN): it has high operational temperature, excellent wear resistance, low fracture toughness, high cost [12].

2.3.2.2   Tool geometry:

The function of tool shoulder and probe is different. In many cases shoulder and pin are made up of different materials and in some cases the tool is constructed from single material. The factors like work material, tool material, joint configuration, process

parameters etc. are required to be considered during tool design and manufacturing. The user's own experience is also to be given importance is designing the tool.

2.3.2.3   CFSW tooling:

A tool with a single shoulder is known as CFSW tooling. A large volume of research papers are published on CFSW covering tool design, its features and effect on weld quality. The basic phenomenon is material displacement due to spinning of tool should be understood, which is explained below.

2.3.2.4   Material flow

The complex flow around the FSW tool can be decomposed into three simpler flow components [28][45]. The component fields, as well as their composite, are incompressible flows. (i) The first one may be considered as a cylinder of the welded material in rigid body rotation separated from the rest of the weld by a cylindrical shearing surface, i.e. a surface of velocity discontinuity (Figure 2.12 (a)). (ii) The second flow component is a homogeneous and isotropic flow field equal and opposite to the welding speed (Figure 2.12 (b)).
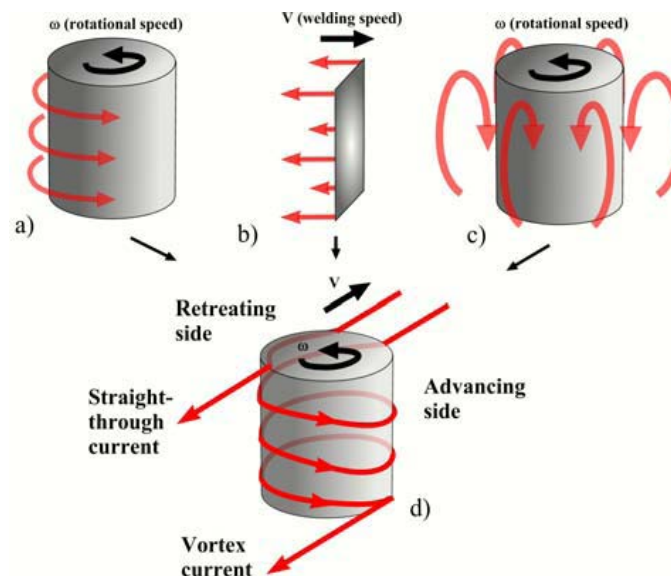

Figure 2.12: Three incompressible flow fields: a) rigid body rotation, b) uniform translation, c) ring vortex, d) combination of the three flow fields [45].

This uniform translation is usually called "extrusion movement" by analogy to the same manufacturing process. (iii) The third component is a ring vortex flow encircling the tool and bringing metal up on the outside, in at the shoulder, down on the inside and out again on the lower regions of the pin (Figure 2.12 (c)). This flow is driven by the threads on the pin. As shown in Figure 2.12 (d), the combination of these three flows results in the formation of straight-through and vortex currents depending on the location.

The Arbegast model [12] treats the FSW as a metal working process that involves five zones: preheat, initial deformation, extrusion, forging, and post weld cool down. These zones are illustrated in Figure 2.13. The work material is heated up when tool rotates is called as preheating. Due to this heat material is softened and initial deformation zone is developed. The material in this zone is forced upward towards shoulder and then downward into the extrusion zone. In this zone material is spinned around the pin from front to rear side where cavity is formed due to pin movement. The heel of the shoulder passes over the material exiting the extrusion zone and forging it. The moment tool displaces and leaves the zone metal is cooled and solid form is left, it is similar to quenching of material during heat treatment.
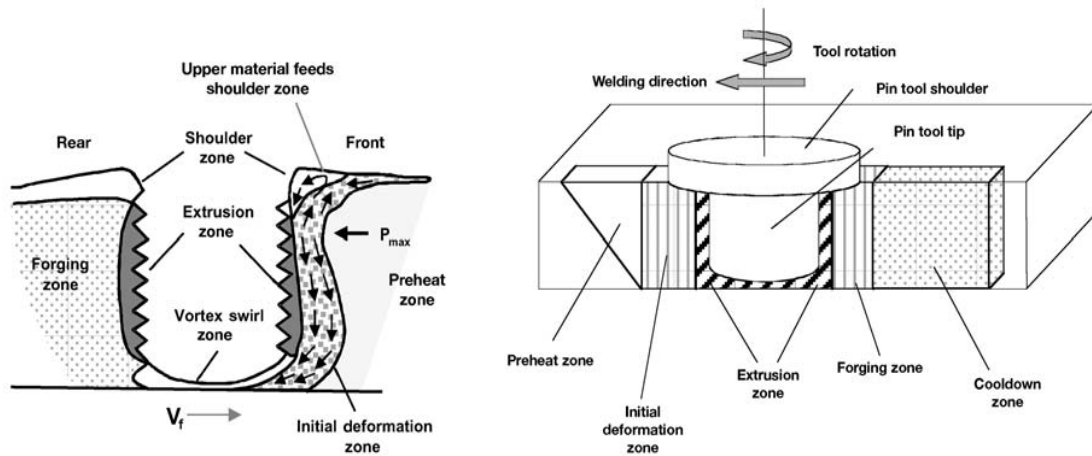

Figure 2.13: Metallurgical processing zones developed during friction stir joining [12]

2.3.2.5   Design of Tool Shoulder and Associated Features

The function of tool shoulder is to heat surface and subsurface regions of the substrate. In thin sheets tool shoulder produces deformational and frictional heat, while pin produces heating in thick workpieces. Hence the most important tool parameter is tool shoulder diameter, as it has direct relation in development of frictional heat.

There is a vast literature available on pin design and its features but limited published literature available for the tool shoulder features [33]. However, according to Mishra and Murray the well-known CFSW has three tool shoulder features in general viz flat, concave and convex as illustrated in Figure 2.14.
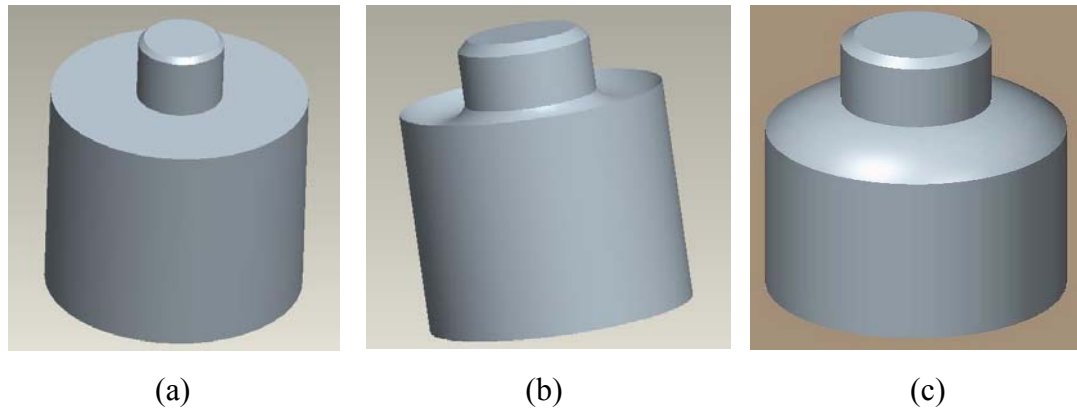

| (a) | (b) | (c) |

Figure 2.14: Shoulder feature (a) Flat (b) Concave (c) Convex.

2.3.2.5.1   Concave shoulders (Figure 2.14 (b))

It was the first shoulder design, commonly referred as standard type shoulder. Concave shoulders produce quality friction stir welds, and is easy to machine and simple in design. The concave shapes that are found in publications and applied by the researchers in their studies are conical and curved [12][46][47]. In the case of concave conical shoulders, the concavity is produced by a small angle between the edge of the shoulder and the pin, typically between 2° and 10° [12]. During the tool plunge, material displaced by the pin is fed into the cavity within the tool shoulder. This material serves as the start of a reservoir for the forging action of the shoulder. Forward movement of the tool forces new

material into the cavity of the shoulder, pushing the existing material into the flow of the pin. To have positive results of this shoulder design, tilting of the tool 2 to 4° from the normal of the workpiece away from the direction of travel is required.

2.3.2.5.2   Convex shoulders (Figure 2.14 (c))

The benefit of having the convex shape is that the outer edge of the tool needs not to be engaged with the workpiece, so the shoulder can be engaged with the workpiece at any location along the convex surface. This shoulder design allows for a larger degree of flexibility in the contact area between the shoulder and workpiece (amount of shoulder engagement can change without any loss of weld quality). This feature configuration improves the joint mismatch tolerance, increases the ease of joining different thickness workpieces, and improves the ability to weld complex curvatures, but the feature arrangement only produces sound welds in thin material. For example the successful studies of convex shoulder welding was reported for welding 0.4 mm sheet with a 5 mm convex tool [12]. To weld thicker material an additional feature known as scroll feature is required on the convex face. A typical example of a shoulder scroll feature is illustrated in Figure 2.11 (b) and 2.15. The importance of the scroll is in its ability to direct material from the outer shoulder into the inner shoulder. Without the scroll feature, the material under the shoulder is pushed away from the weld zone and appears at the flanks of the shoulder in the form of flash [46][48].
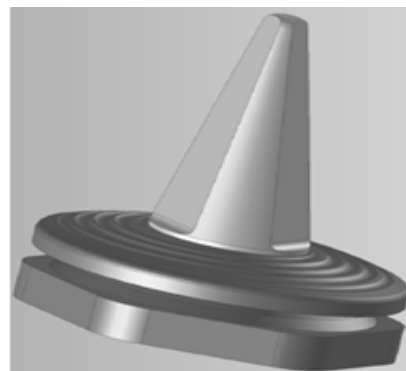
(a)   (b)

Figure 2.15: Convex scroll shoulder [12][49]

Flat, concave and convex shoulders can contain other additional secondary features to generate heat and induce material deformations which are aimed at producing better material mixing and weld quality. These potential features are presented in Figure 2.16. Although there is a range of additional secondary feature designs for the shoulder, the most common shoulder feature used in the previous and current studies was a scrolled shoulder [12][33][46][47][50]. Dawes and Thomas [48] studied the feasibility of different shoulder features as shown in Figure 2.16.
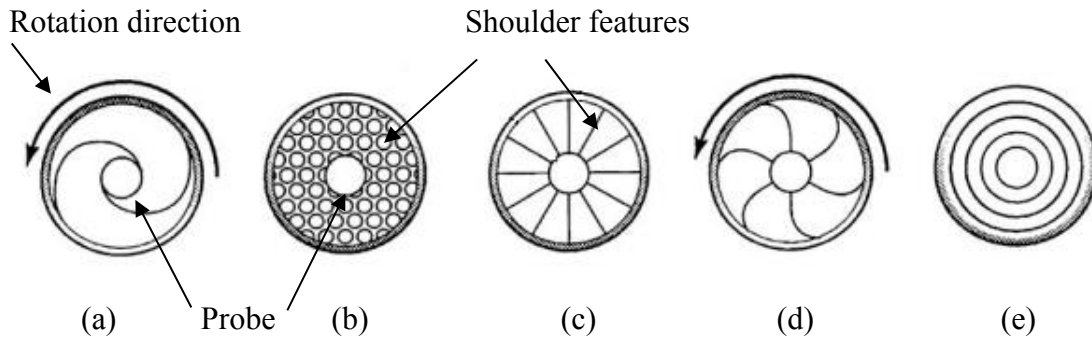

Figure 2.16: Different design of shoulder features (a) scrolls (b) knurling (c) ridges (d) groove (e) concentric [12]

Besides these secondary shoulder features, fillet and chamfer features have also been applied on the shoulder edges in conjunction with the flat surface shoulder as shown in Figure 2.17. Both were found to produce good welds. The presence of fillet contribute to a smooth weld surface and help to minimize the amount of flash [33][51]. The published paper does not include the size of the fillets or chamfers that were used.
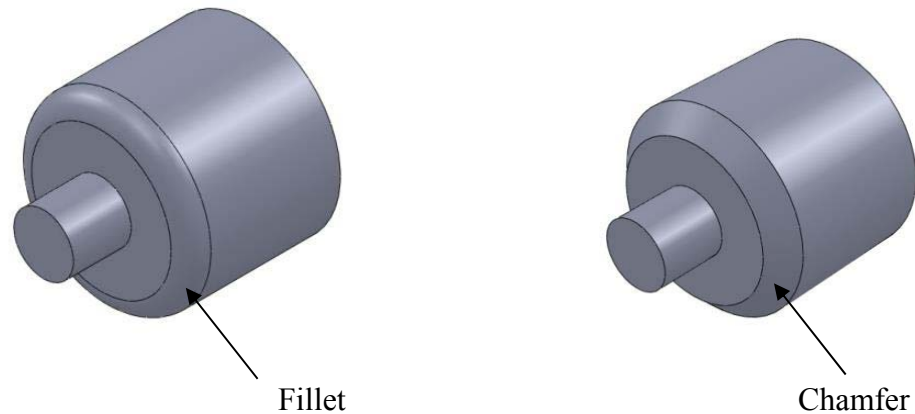

Figure 2.17: Fillet and Chamfered tool shoulder.

Underlying the secondary features applied to the FSW tool, the success of producing sound welds is primarily linked to the amount of heat generated and workpiece material flow induced by the tool.

Based on Arora et al. [52] studies, the flow of material has "sticking and sliding" phenomenon observed at the tool workpiece interface in FS welding. Hence proper tool dimensions need to be selected. In general shoulder diameter to work thickness ratio is considered to be 3:1.

A clear trend is observed by Dubourg et al. [45] that the shoulder diameter is about 2.3 times the sample thickness plus a constant of 7 mm. It was derived from the 30 different set-ups reported in the literature (aluminium samples in butt configuration from 1 to 8.3 mm thick).

2.3.2.6 Design of Tool Pin and Associated Features

The pin functions to heat generation through friction, material deformation and circulating the softened material, as it is fully penetrated in the work material and has full contact to the material surface. Also it govrns the deformation depth and welding speed.

Based on the published literature, some flash light following designs and their merits and limitations are illustrated.

As illustrated by Mishra and Mahoney [12], commonly used pin designs are as follows:

2.3.2.6.1 Round-bottom cylindrical pin (Figure 2.18 (a))

A round end to the pin tool facilitates easy plunging of tool even if predrilled hole is not there in the workpiece. The quality of weld root underneath the bottom of pin is also improved. The best dome radius was specified as 75% of the pin diameter. Whereas the quality immediately below the pin is affected with decrease in the dome radius. The stress concentration at the root of threads is eliminated with a radius at the bottom of the threads and will increase tool life.

2.3.2.6.2   Flat-bottom cylindrical pin (Figure 2.18 (b))

The friction velocity of a rotating cylinder increases from zero at the center of the cylinder to a maximum value at the edge of the cylinder. The local velocity coupled with the friction coefficient between the pin and the metal dictates the deformation during friction stirring. The lowest point of the flat bottom pin tilted to a small angle to the normal axis is the edge of the pin, where the velocity is the highest.
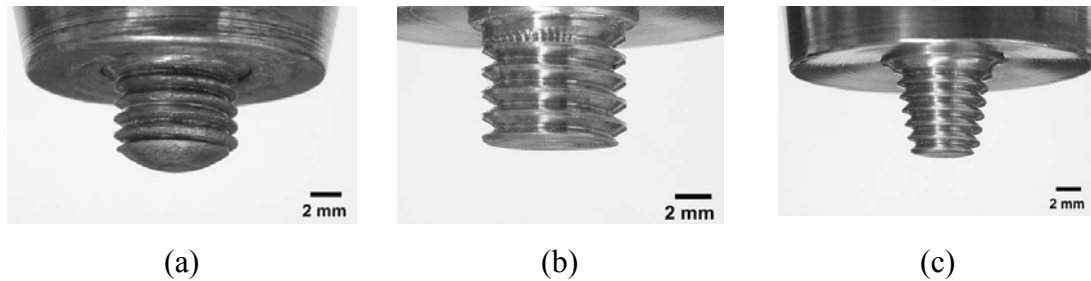

| (a) | (b) | (c) |

Figure 2.18: Commonly used tool pin designs (a) round bottom, (b) flat bottom,
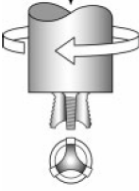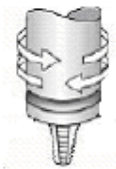(c) truncated cone [12]

2.3.2.6.3   Truncated cone pin (Figure 2.18 (c)):

For less thickness say up to 12mm, a cylindrical pin design will serve the purpose to weld aluminium material. But for higher thickness and faster welding speeds a little modification in the form of truncated cone shape is better. Truncated cone pins have lower transverse loads (when compared to a cylindrical pin), and the largest moment load on a truncated cone is at the base of the cone, where it is the strongest [12].

Thomas et al., presented their research on FSW tool design which was conducted in TWI in early 2003. Their designs are summarized in Table 2.2 [8][42]

In the first column, a cylindrical tool with a threaded pin with a frustum shape is stated to be suitable for butt joining where it produces satisfactory weld on plate components. Likewise tapered (also known as conical) threads in the Whorl and MX triflute designs (columns 2 and 3 of Table 2.2) induce a vertical component of weld material velocity that facilitates plastic flow and have been successfully used in butt welding.

Table 2.2: Tools designed at TWI [8][42]

Tool	Cylindrical	Whorl ™	MX triflute™	Flared triflute™	A-skiew™	Re-stir™
Schematics						
Tool pin shape	Cylindrical with threads	Tapered with threads	Threaded, tapered with three flutes	Tri-flute with flute ends flared out	Inclined cylindrical with threads	Tapered with threads
Ratio of pin volume to cylindrical pin volume	1	0.4	0.3	0.3	1	0.4
Swept volume to pin volume ratio	1.1	1.8	2.6	2.6	Depends on pin angle	1.8
Rotary reversal	No	No	No	No	No	Yes
Application	Butt welding; fails in lap welding	Butt welding with lower welding torque	Butt welding with further lower welding torque	Lap welding with lower thinning of upper plate	Lap welding with lower thinning of upper plate	When minimum asymmetry in weld property is desired

While the flute feature in *MX* triflute and Flared triflute (columns 3 and 4 of Table 2.2) is stated to increase interfacial area or stirring action between the tool and workpiece leading to increased heat generation rates, softening and flow of material. Consequently, it is evident that more intense stirring reduces both the traversing force for the forward tool motion and welding torque. Moreover in the review paper by Nandan et al. [53], a Triflute tool with a tapered pin feature produced a strong auguring action and thus increased the downward force. The associated stirring action can also be induced by inducing flat features on the pins which will be discussed later in this section.

Cylindrical, Whorl and MX triflute tools are best for butt welding but not for lap welding. This is because, the plunge force causes excessive thinning of the upper plate which then causes the adhesion of oxide in between the overlapping surfaces. In solving this issue,

Flared triflute, A-skew and Re-stir tools were design by TWI that have higher swept volume which then expands the stir region resulting in a wider weld area. The Re-stir tool has an additional advantage whereby it applies periodic reversal of tool rotation thus eliminates inherent asymmetry in microstructures flow [42][53]. These tools are commercially available, but the complete understanding of each tool feature is not wholly exposed. Further studies and results sharing have been undertaken by other researchers with the aim of understanding the effects of secondary features on tools as follows.

As compared to plain cylindrical pin, a tapered pin tool has more uniform stress and lower frictional contact, which results in reduction in torque and bending moment on the tool [25]. Zhao et al. [54] studied the use of tapered and cylindrical pins with and without a thread for welding Al 2014 (butt joint of 6 mm thickness). The dimensions of the tapered pin were 8 mm for the major diameter and 6 mm for the minor diameter. Figure 2.19 presents the tools used in their studies. The observations are that the quality welds were through the tapered and screwed pin. However, using a plain cylindrical and tapered tool pin, the mixing of material was not so effective and hence void defects resulted in weld region.

(a)   (b)   (c)   (d)

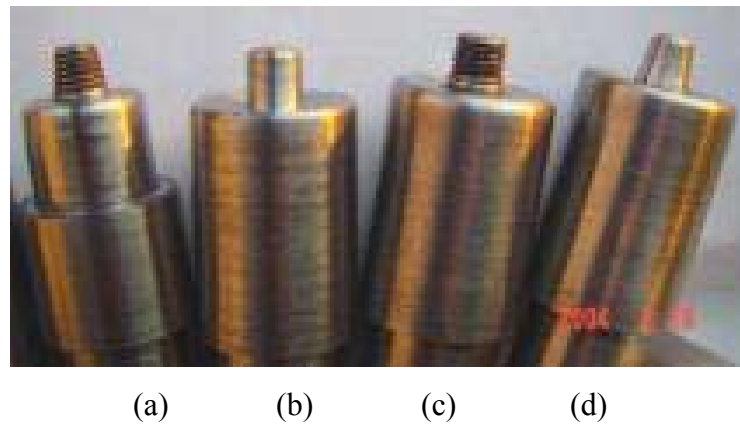Figure 2.19: Image of CFSW tools (a) Tapered thread cylindrical pin (b) Straight Cylinder (c) Threaded cylindrical pin (d) Tapered cylindrical pin [54]

A similar experiment was performed by Sree Sabari et al. [55] on AA2519-T87; a new armour grade aluminium alloy employed in the fabrication of light combat military vehicles. The experiment was done in air and underwater using four different tool pins

(see Figure 2.20). From this investigation, it is found that the joint made by taper threaded pin profiled tool underwater cooling medium exhibited higher tensile properties of 345 MPa and joint efficiency of 76 %. The enhancement in the strength is attributed to the precipitation hardening, grain boundary strengthening and narrowing of lower hardness distribution region (LHDR).
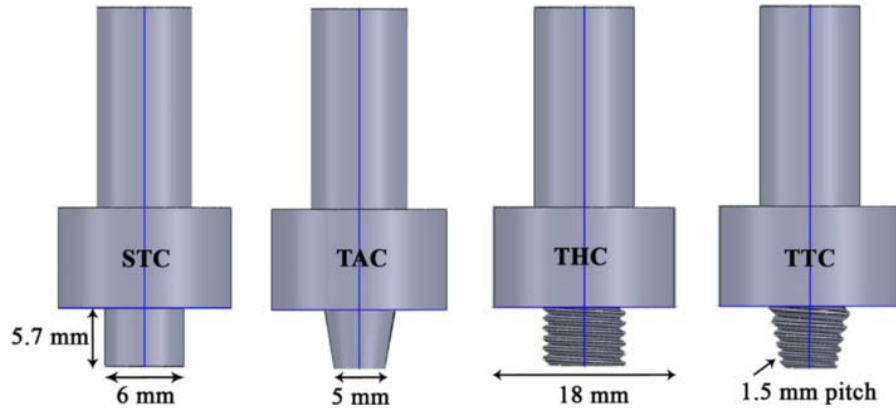

Figure 2.20: Dimensions of the tool pin profiles: straight cylindrical (STC), taper cylindrical (TAC), straight threaded cylindrical (THC) and taper threaded cylindrical (TTC) [55]

McClure et al. [56] did studies on threaded featured tools with 14, 20, 32, 48 TPI (threads per inch) of cylindrical pin in welding of 6mm thick of 6061-T6 Aluminium alloy with butt joint configuration. They found that the thread induced material "flow up and down in the weld region". Plain or unthreaded pin provides insufficient vortex flow while lower pith threaded pin has large scale top to bottom flow of material in weld area. The presence of the thread feature normally resulted in a conforming defect free weld.

Radisavljevic et al. [57] developed two different friction stir tools having a little variation in pin threads, i.e., use of regular (tool 310) or rounded (tool 310-O) threads, Figure 2.21. The tools are made of tool steel, with spiral thread on the 5.5 mm length conical pin and concave shoulder. Taper screw thread pins are designed, with thread slope of 5 degrees and diameter on root and head of 10 and 4 mm, respectively. Pins have an angle of 20 degrees. Pitch of the thread is 1.5 mm. The investigation showed that the welded joints were defect free having good mechanical properties and excellent surface appearance.
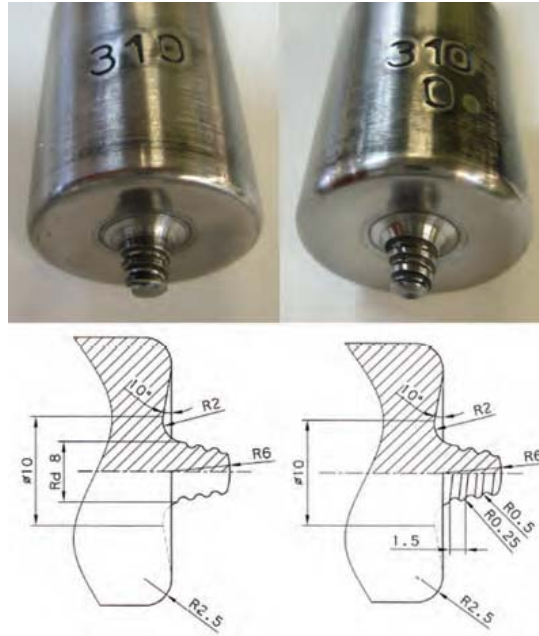
Figure 2.21: FSW tools with regular and round spiral threads [57]

Furthermore, Elangovan and Balasubramanian [3] in their work introduced pin features with flat faces (square and triangular) which were found to have better material dynamic swept volume compared to a cylindrical pin. As shown in Figure 2.22, they used five different tool pins in butt joint welding of AA6061 aluminium alloy 6 mm thickness.
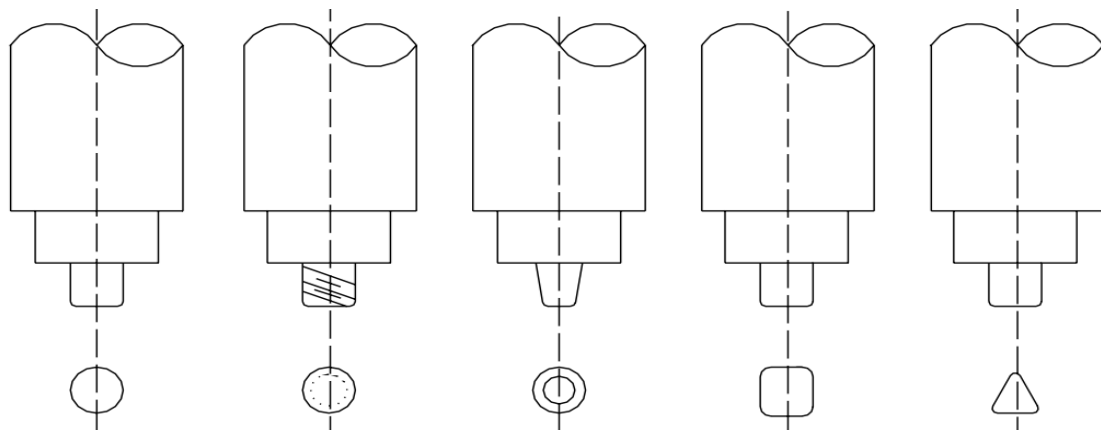

Figure 2.22: CFSW pin tool (a) Straight cylinder (b) Threaded cylinder (c) Tapered cylinder
(d) Square (e) Triangle [3]

The diameter of the pins was 6 mm. They found from the weld macrostructure observation that square, threaded cylinder and triangular secondary pin features produced

31

defect free weld regions. Furthermore, in tensile tests, it revealed that the joints fabricated by the square pin (four flat) feature exhibited superior tensile properties followed by the triangular, threaded cylinder and tapered pin features. The straight cylinder pin produced the lowest tensile result, whereby the tensile strength was around 50% of the parent material.

Parallel to this study, Padmanaban and Balasubramanian [58] used the same pin features in joining AZ31B, a Magnesium alloy. The joint was a butt joint configuration of 6 mm thickness plate. A different finding was found whereby the optimum tool was the cylindrical threaded pin feature which yielded defect free and a fine grained nugget region. Both triangular and square pins produced defects in the nugget region which was believed to be due to insufficient heat generation and a large amount of metal swept from the stir zone.

Vijay and Murugan [50] studied the more flat faces than Elangovan. They also have considered the shoulder to pin diameter ratio (D/d). They used a 16 mm shoulder diameter for butt joint welding of 6 mm thick metal matrix composite (MMC) Al-10 wt.% TiB_2. They adopted three D/d ratio (2.8, 3.0 and 3.2) and three features (four, six and eight flat faces) as shown in Figure 2.23. Joints welded by the square pin feature tools exhibited high tensile strength as compared to other features [59]. This type of tool was similar to what had been suggested earlier. When a tapered square pin feature was introduced to the parallel square pin, it formed a joint with the least tensile strength. Other pin features did not change significantly. Vijay et al. [50] stated that the square pin feature produces 133 pulses/s and hexagonal pin profile produces 200 pulses/s, when the tool rotates at a speed of 2000 rpm. This shown that there is not much pulsating action differences especially for the octagonal pin profiled tool due to the small flats. It is just replacing plain cylindrical pin tool. In the case of tapered pin tools, less material was being swept as compared to that for a straight square pin tool, the associated joint exhibited less tensile strength. This was also reflected by the microstructure images whereby bigger grains were evident which accounted for the poor tensile strength in joints made using taper pin tools.

Figure 2.23: Tools with different amount of flat faces [50]

In the studies conducted by McClure, et al. [56], it is indicated that typically the diameter of tool pin is equal to the thickness of the materials to be welded and its length should be slightly shorter than the thickness of the material to be welded. These claims are also supported by other researchers' findings [3][4][54][58] whereby the diameter of pin is equivalent to the thickness of the welded part, for producing a sound weld. As far as the pin length is concern researchers have suggested a value 0.2 mm to 0.3 mm smaller than the sheet thickness [4][58]. However some researchers used tool dimensions other than mentioned in the literature and could succeed to have quality weld. In many cases researchers did not mention the pin dimensions [60]. The reasons for quality weld are because of other significant welding parameters such as dwell time, axial force and plunge depth, being well optimized for these specific applications [3], and the variable process parameters like rotational speed and traverse speed are properly selected.

2.3.2.6.4   Different types of CFSW tool probe design

The tool pin shapes and their main features can be summarized as shown in figure 2.24 [61]. The end shape of the probe is either flat or domed. The flat bottom probe design that emphasizes ease of manufacture is currently the most commonly used form. The main disadvantage of the flat probe is the high forge force during plunging. In contrast, a round or domed end shape can reduce the forge force and tool wear upon plunging, increase tool life by eliminating local stress concentration and improve the quality of the weld root directly at the bottom of the probe.
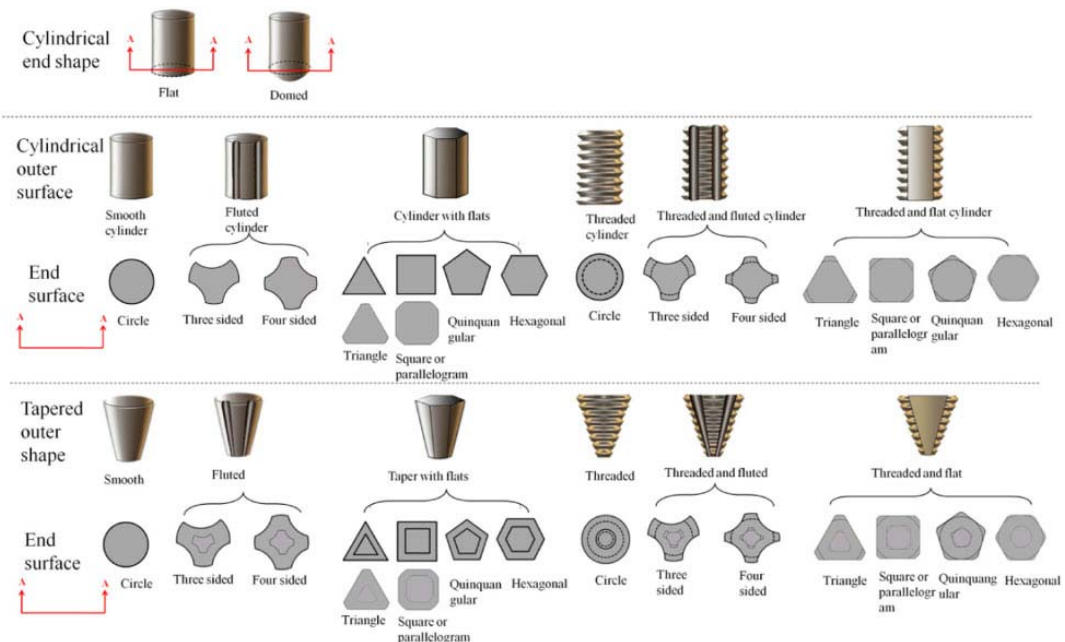
Figure 2.24: The tool pin shapes and their main features for CFSW [61]

2.3.2.7   FSW tool design is characterized by the following parameters

➤ Shoulder diameter: Excessively wide tool diameter can sweep surface oxide into the weld resulting in entrapped oxide defects.

➤ Pin diameter: The volume of material stirred during FSW is proportional to the diameter of the tool pin.

➤ Pin length: Too short pin may result in root flaws while excessively long pin could damage the tool or backing plate [12].

- ➢ Pin shape: Cylindrical and tapered tool pins are common, but are not effective in avoiding weld defects such as worm-holes [53][62].

- ➢ Pin angle: Pin angle is the angle between the conical surface of the pin and its axis.

- ➢ Increasing pin angle leads to more uniform temperature distribution along the vertical direction and may help reduce distortion [53][63].

- ➢ Pin threading: Threaded tools generate more heat and improve vertical mixing of the material because they exert higher downward forces in comparison with unthread cylindrical and tapered tools [53][64].

Zhang et al. found that there must be a relation between pin diameter and shoulder diameter and plate thickness for heat generation and proper material transport [61]. They did experiment for both similar and dissimilar welds, produced using several alloys and materials. As shown in Figure 2.25(a), the author shows that the ratio between the pin (D_p) and shoulder (D_s) diameters follows the expression,

$$Ds = 2.097Dp + 4.760 \tag{2.2}$$

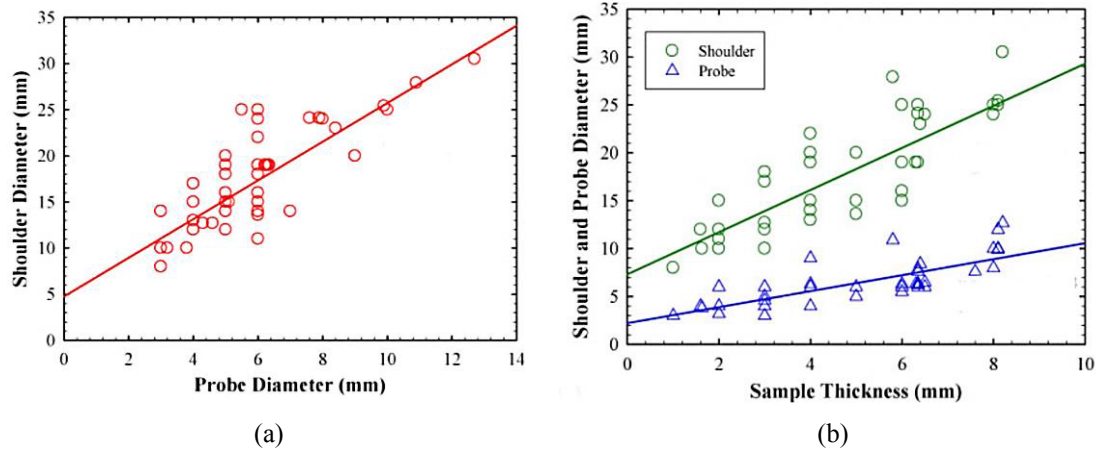(a)   (b)

Figure 2.25: Ratio of pin and shoulder diameter: (a) Pin (Probe) diameter versus Shoulder diameter, (b) thickness versus shoulder and pin diameters. [61]

Furthermore, plotting the pin and shoulder diameter values versus thickness, which is shown in Figure 2.25(b), the author developed the following relations,

$$Ds = 2.199t + 7.318 \tag{2.3}$$

$$Dp = 0.834t + 2.224 \qquad\qquad\qquad (2.4)$$

According to Deqing et al. [65] there is a correlation between the radius of the shoulder and the radius of the pin, i.e. a 3 to 1 ratio. This means that the radius of the shoulder is three times the radius of the pin. Dubourg [45] state that the diameter of the shoulder is related to the thickness of the plate:

$$d_{shoulder} = 2.26 * t_{sheet} + 6.99 \qquad\qquad (2.5)$$

These two statements claim that pin and shoulder diameter can be easily decided once the thickness of the plate is known, in order to achieve a good weld.

It is also important to emphasize that the assessment of the ideal tool dimension is being mainly based on trial and error method for a restrict range of pin and shoulder diameters. No appropriate principle for the determination of an optimum shoulder and pin diameter was established until now. As mentioned by Rai et al. [66] the search of this principle is just beginning.

According to Rai et al. (2011) [66], during the process, the tool is subjected to severe stresses and wear at high temperatures. The tool life depends mainly on hardness of the base material. From an industrial perspective, tool life constitutes a key factor in process cost/efficiency. Depending on the material to be welded an optimization of tool geometry and tool material is required in order to increase the tool life for definite weld quality.

2.3.2.8 BFSW tooling

Though the idea of bobbin tool was collectively patented by TWI, within the general FSW process, in 1991[25], since its inception very lean literature has been published about bobbin FSW as compare to CFSW. The BFSW is identified by three primary features; the upper shoulder, a pin and the lower shoulder. The design concept is an extension of the CFSW tooling with one additional shoulder connected to the pin on the bottom surface of the plate to be welded.

Schneider et al. [29] used cylindrical threaded secondary pin features in their studies on butt welding 0.357 inch thick AA2195-T87 Aluminium Alloy panels. The tools were prepared in two different diameter sizes that were 0.5 inch and 0.327 inch with each of the tools having 0.12 inch and 0.07 inch thread pitch. In their studies, the travel speeds were set at 11 ipm and 14 ipm with varied spindle speeds. For the experiment runs using travel speed of 11 ipm, the spindle speeds were increased from about 10 rev/in to 35 rev/in. Meanwhile for 14 ipm the spindle speeds were increase from 7 rev/in to 16 rev/in. From their experiment results it is believed that BFSW is capable of producing sound welds, and no reports found on weld defects in their studies. But it is recorded that the nugget bulge size increased as the spindle speed and tool diameter increased. The nugget bulge eventually affects the welded material by reducing the ultimate strength.

Furthermore, previous researchers recommended the use of a cylindrical tapered pin tool for the BFSW process. Tapered pin provides uniform stresses in the tool, because less material is displaced during welding. In addition, the use of a tapered pin enables a proportional reduction in the diameter of the lower shoulder of the bobbin tool. The decrease of lower shoulder diameter results in lower frictional contact and plunging resistance, therefore less torque and bending moment on the tool which can minimize or eliminate the chances of tool failure. To improve the volume of swept material by the tapered pin; researchers recommend three flats features to be applied on the pin. This tool design was used in butt joint welding of 8 mm thick, 12% Chromium alloy steel, and was found to be successful in producing good weld [25]. There are no record regarding welding process loads by the researchers in BFSW [25][29].

Studies undertaken by Threadgill et al. [13] used a combination of cylindrical, thread, three flats and taper on the pin with smaller diameter on bottom tool shoulder. The studies focused on welding 25 mm thick AA6082-T6 Aluminium Alloy in a butt joint configuration. The tool used in this study, along with its specifications is shown in Figure 2.26. Torque and forces values were recorded. The welding results revealed that the traverse force and torque load produced by this tool is similar with CFSW; 11kN and 400 Nm respectively. Higher values of force and torque would naturally be expected if a tapered pin and small lower shoulder were not used. For the axial force the bobbin tool

produced 14.73 kN which is much lower than that found when using conventional tools (in their work, the conventional tool features was not mentioned). In addition to their findings, they found a clear boundary of macrostructure was produced in the weld.

Figure 2.26: BFSW tool used by Threadgill et al. [13] to weld 25 mm thick, AA6082-T6 Aluminium Alloy.

There is reduction in heat generation when a gap is there in shoulder and plate surface, which ultimately welcome weld defects. A scrolled shoulder combined with a convex feature was found to be successful in the BFSW application and also found to be the case for CFSW (see the CFSW tooling section). Despite this revelation, there are researchers using flat or flat with scrolled shoulder in their studies and still capable of producing defect free welds, perhaps due to the tightly controlled and optimized other covert parameters [13][29].

Sued has worked extensively on bobbin tool. He has developed different tools assembled and fixed bobbin. He has applied for patent for insert type bobbin tool having secondary features on shoulder, which was found otherwise difficult to be developed in case of fixed bobbin tool [67]. The researcher also studied the effect of gap on quality of weld. He used threaded pins with different pitch and flats provided on the pin. He found in his initial study that, the pin with four flats feature produced a sound weld for thin plate aluminium. The limitation of this study was the experiment was carried weld-on-plate [68].

2.4 MICROSTRUCTURAL EVOLUTION AND TEMPERATURE DISTRIBUTION

To have changed microstructure of a material, the friction stir welding process can be used. Heat and deformation helps improve microstructure in FSW. This is possible because of rotation and linear movement of the tool resulting in very fine refined equiaxed structures in the weld regions as compare to base metal.
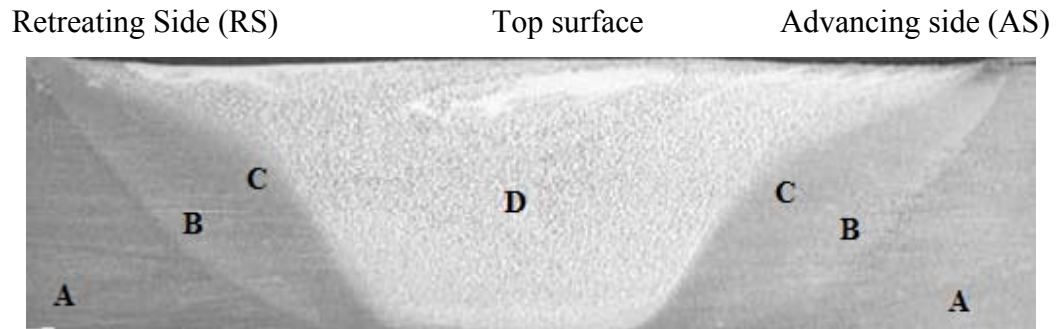
The mechanical properties and microstructures are different in the different zones or regions developed in the FS welds. It is dependent on the frictional heat and deformation in the region. The weld region comprises of the area directly beneath the tool shoulder. The width of the weld region is approximately equal to tool shoulder diameter as shown in Figure 2.27. The weld region is narrower at the bottom due to less influence from the tool shoulder and the tapering of the probe. However, this is not always the case, other variants of FSW processes and every different design of tool will create a differently shaped weld region but they contain the same features. The weld region in FSW can be divided into three zones [8][12], in order to differentiate them from the unaffected parent metal (base metal). These zones are; heat affected zone (HAZ), thermo-mechanically affected zone (TMAZ) and the weld nugget zone (also referred to as the stirred zone). Each weld zone is shown in Figure 2.27 (a) for CFSW and Figure 2.27 (b) for BFSW. By referring to Mishra and Ma [12], these zones are defined as-

Parent metal: This is material remote from the weld that has not been deformed and that, although it may have experienced a thermal cycle from the welding process, it is not affected by the heat in terms of microstructure or mechanical properties.

TMAZ: In this region, the FSW tool has plastically deformed the material, and the heat from the process has also exerted some influence on the material.
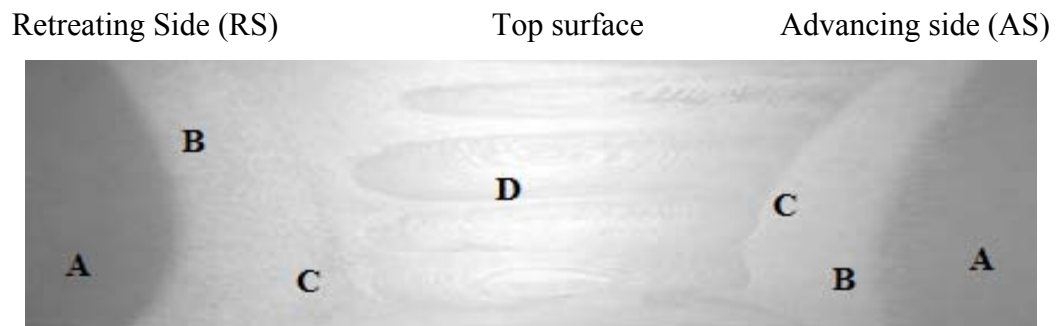
Weld nugget zone: The fully recrystallized area, sometimes called the stir zone, refers to the zone previously occupied by the tool pin. The term stir zone is commonly used in friction stir processing, where large volumes of material are processed.

HAZ: In this region, which lies closer to the weld center, the material has experienced a thermal cycle that has modified the microstructure and/or the mechanical properties. However, there is no plastic deformation occurring in this area.

Retreating Side (RS)   Top surface   Advancing side (AS)

Bottom surface

(a)

Retreating Side (RS)   Top surface   Advancing side (AS)

Bottom surface

(b)

A = Parent Metal, B = Heat affected zone (HAZ), C = Thermo-mechanically affected zone (TMAZ),

D = weld nugget.

Figure 2.27: FSW macrostructural cross section of 6082-T6Alluminium alloy in butt joint welded form, (a) CFSW (b) BFSW [24]

As shown in Figure 2.27, CFSW and BFSW have different region sizes and forms. For example, by referring to the weld nugget zone, CFSW inherited the basin shaped nugget while the BFSW weld nugget zone adopts the form of an hour-glass [8] [29]. It is found in both FSW processes, the size of nugget area decreases towards the center, and for the BFSW process this area widens again towards the lower surface. This is because the pin diameter is smaller than the shoulder diameter.
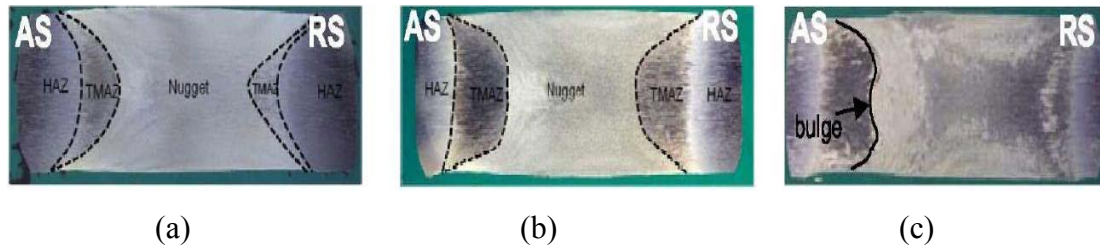
Figure 2.28: Variations in BFSW weld nugget zone as the tool rotation is increased, (a) curve form
(b) flatten form (c) nugget bulge [29]

The microstructure regions, sizes and forms are evolved depending on dynamic recrystallization (continuous tool stirring and tool travel). For example, when the tool spindle speed is increased at constant traverse speed, the center weld nugget region edges change from the natural curve form (Figure 2.28 (a)) to flatten edges along the center (Figure 2.28 (b)). A radial bulge then emerged at the stage when the highest spindle speed was reached (Figure 2.28 (c)). This then effects the natural HAZ location and displace it radially away from the weld nugget zone [29].

The dynamic recrystallization is also related to the heat generation (temperature) which not only affects weld zone forms and shapes but also grain sizes. Grains in FSW are in the micron range and the sizes grow proportionately with the increment of heat generated during the process. Figure 2.29 shows the temperature distribution on a welded plate in CFSW. The peak temperature was found at the weld nugget area and decreased as the location is further away from the stirring area. By comparing the advancing and retreating side, the Advancing side generally has higher temperatures than retreating side because of the forging effect produced by the tool shoulder.
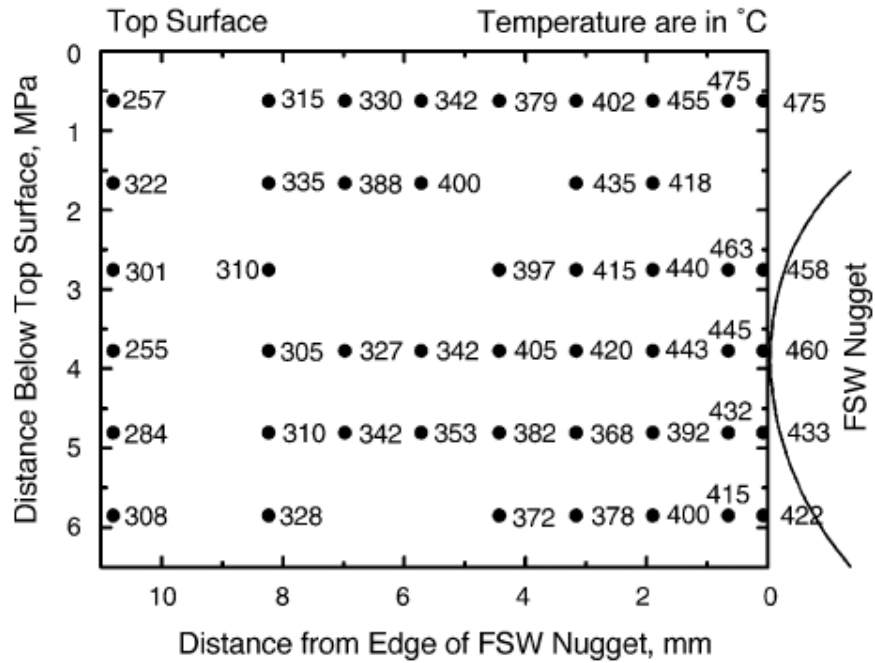
Figure 2.29: Temperature distribution adjacent to a CFSW in 7075Al-T651 [69]

In terms of grain size, coarse grains are found at the zone that has the highest temperature and slowest cooling effect while finer grains are found when active cooling takes place.
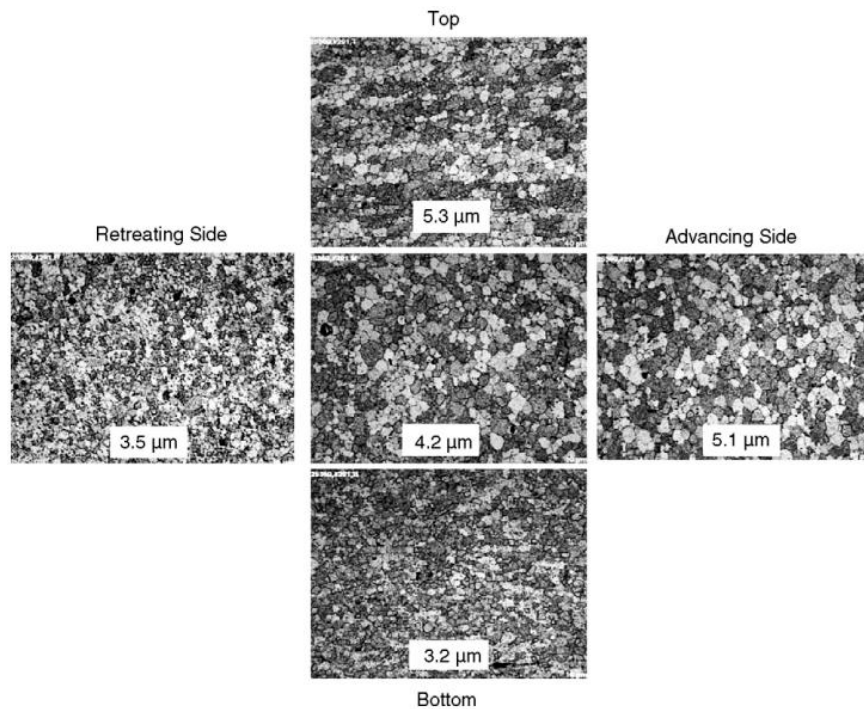

Figure 2.30: Grain size distribution for CFSW in various location of 7050 Aluminium [8]

Figure 2.30 shows the grain size distribution in FSW. The average range of grain sizes recorded by the researchers in CFSW are between 2 μm to 22 μm but at the weld nugget area the grain size ranges from between 2 μm to 6 μm [8][11][70] regardless of material type.

For BFSW, the higher temperature produced by the double acting shoulder (when compared to CFSW) and passive cooling rate results in coarse grains. This is proven by the studies done by Neumann, et al. [71] when they detected that the peak temperature produced by bobbin tools is higher than that for conventional tools when welding 2024-T351 alloy. The researchers also found that RS had a higher temperature when compared to AS which was opposite to the findings for CFSW. Furthermore, in Threadgill, et al. [13] studies, they mention that the grain sizes at the weld nugget area were in a range from 6 μm to 8 μm and the grain size distribution was uniform (due to uniform heat supplied by the tool) in comparison to a varied grain size from the top to the bottom of CFSW tool welds.

A substantial grain refinement of an aluminium matrix (AA7005) composite reinforced with 10 vol.% of Al_2O_3 particles was observed by Ceschini et al. [72]. It was due to dynamic recrystallization induced by the frictional heating and plastic deformation during welding. The average grain size of the matrix alloy was about 30 μm in the base material, while decreased up to 12 μm in the nugget zone of the FSW (Figure 2.31).
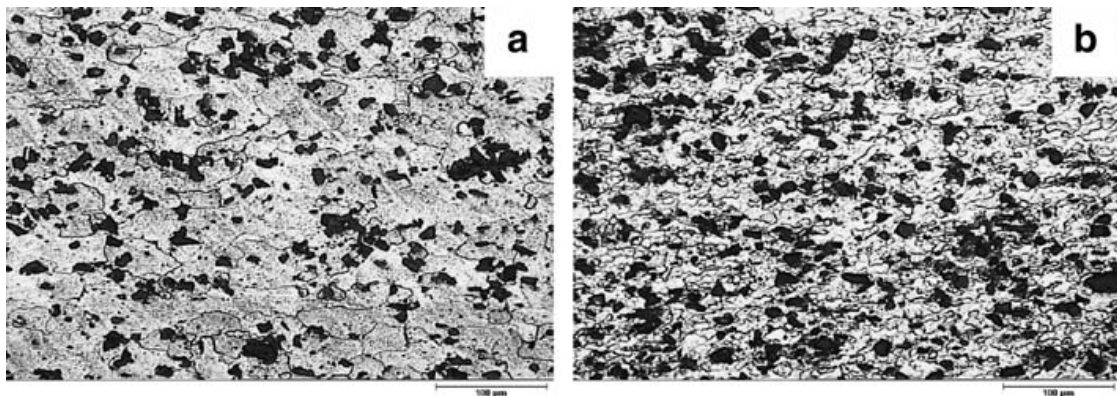

Fig. 2.31: Effect of the FSW on the aluminium matrix grain size: (a) base material and (b) nugget in the FSW zone. [72]

Cavaliere and Squillace [73] during welding dissimilar al alloys AA6082 and AA2024, observed a completely recrystallised structure in the joints with AA6082 on the advancing side while not completely recrystallized structure observed in one joint welded with AA2024 on the advancing side.

2.5 WELD PROPERTIES

Material properties such as mechanical and corrosion behavior are modified when subjected to material deformation and different thermal exposure in the FSW process. It is noted that based on the review paper by Mishra and Ma [8] the distribution of stress, hardness, strength and ductility exhibited an "M" like distribution across the weld. For example this distribution is shown in Figure 2.32 for the residual stress in CFSW of 6013Al-T4.
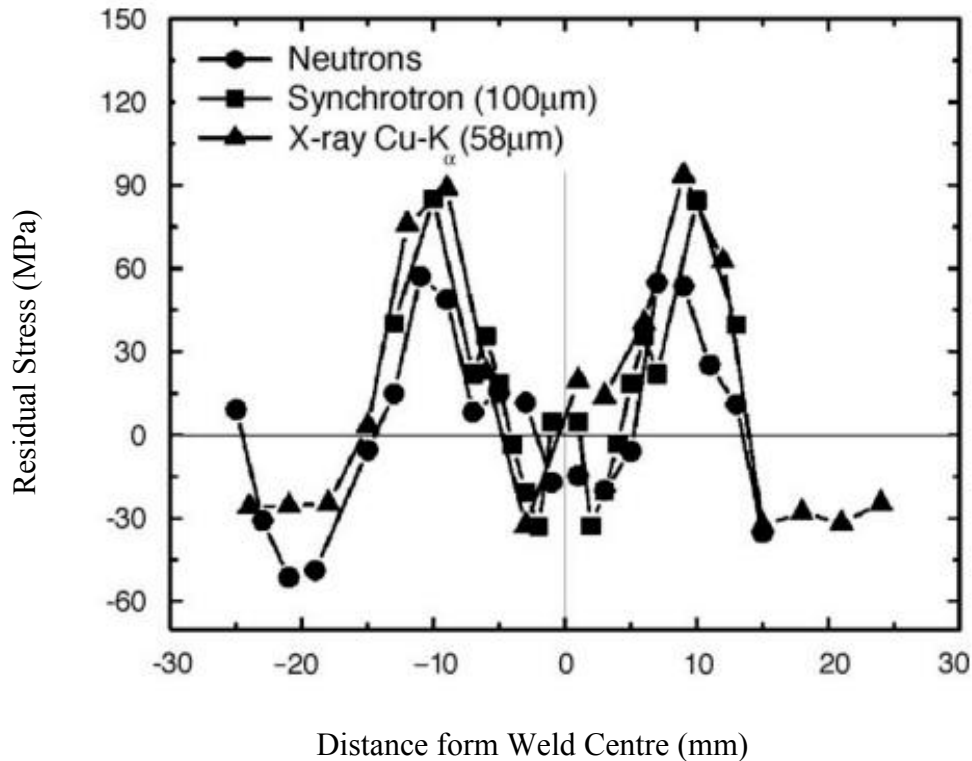

Figure 2.32: Longitudinal residual stress distribution in FSW 6013Al-T4 welds determined by different measurement methods [74]. Sample welding parameters: tool rotational speed: 2500 min-1; Welding speed: 1000 mm s-1; tool shoulder diameter: 15 mm

FSW a solid state process does not reach to melting point of weld material and hence has lower residual stress compare to fusion welding. However, due to fixing of weld plates higher clamping forces are exerted on weld materials. These restraints impede the contraction of weld nugget and HAZ during cooling cycle, resulting in the generation of longitudinal and transverse stresses.

The findings of residual stress evolution studies founded by CFSW researchers are as summarized:

(a) In the transition between the fully recrystallized (weld nugget zone) and partially recrystallized (TMAZ-HAZ zone) regions, the residual stress is higher than that observed in other regions of the weld. The longitudinal (parallel to welding direction) residual stresses were tensile and transverse (normal to welding direction) residual stresses were compressive. The low residual stress in the FSW welds is attributed to the lower heat input during FSW and recrystallization accommodation of stresses [75].

(b) The longitudinal residual stresses are always higher than the transverse and independent of pin diameter, tool rotation rate and traverse speed. But Nandan et al. [53] stated that the longitudinal stress is dependent on traverse speed, because higher stress is measured when the travel speed is increased.

(c) Although in an earlier paragraph in this section it was mentioned that the stress distribution exhibited an "M" like distribution, it was suggested that the transverse residual stresses exhibited a peak at the weld center [74].

(d) The increase of tool rotation rate at a constant traverse speed did not exert marked effect on the residual stress distribution but slightly widened the stress range. The longitudinal residual stress varied only slightly with depth, whereas the transverse stress varied significantly through the thickness. "The sign of the transverse residual stress near the weld center line is in general, positive [tensile] at the crown and negative [compression] at the root" [76].

(e) The magnitude of residual stress in FSW is different for different materials [8]. These stresses are important because the condition of the stress gives practical impact on the fatigue properties and other mechanical properties of the welded plate. This is supported by the fact that most weld defects occur at the TMAZ, HAZ and TMAZ/HAZ interface [8][51][58][77].

The inherent internal stresses are believed to be reduced when the bobbin tool is used in FSW because of minimal axial and plunge forces which avoid the requirements of rigid clamping and high plunge forces.

A detailed study was conducted by Lafty et al. [78] on 4 mm butt joining of three different heat treated (tempered) states of AA6056 alluminium alloy (T4, T6 and T8). In this study a comparison between CFSW and BFSW was made and the impact of these processes on mechanical properties of the welded plate was observed. From their work it was found that the hardness, as shown in Figure 2.33, was higher for CFSW than BFSW (measurements were made at three different heights in the weld: top surface, middle surface and lower surface).

Distance form Weld Centre (mm)
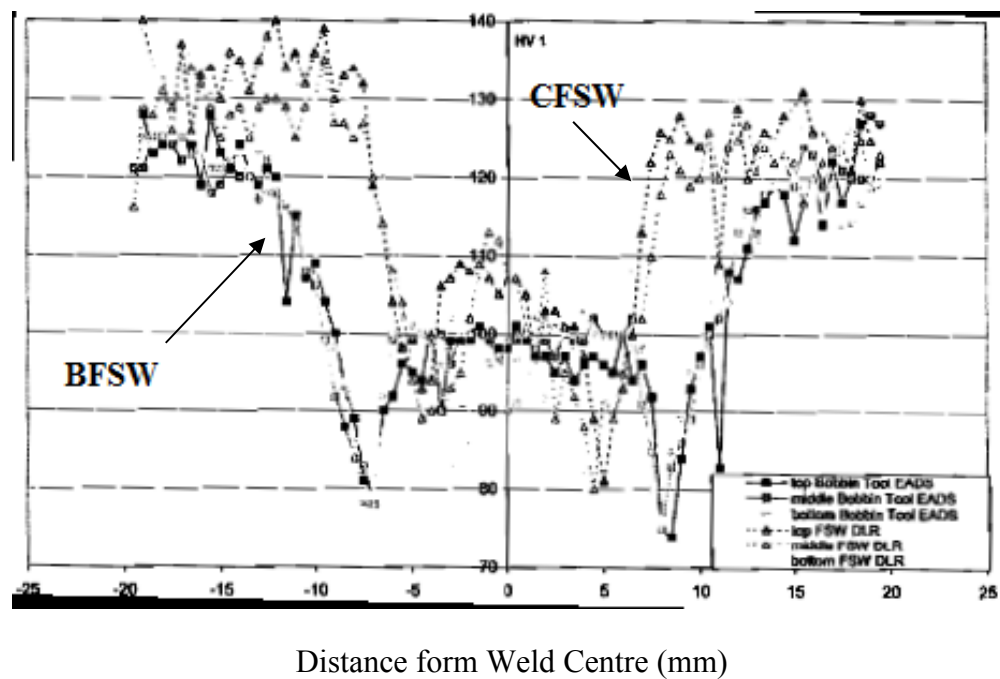
(a)
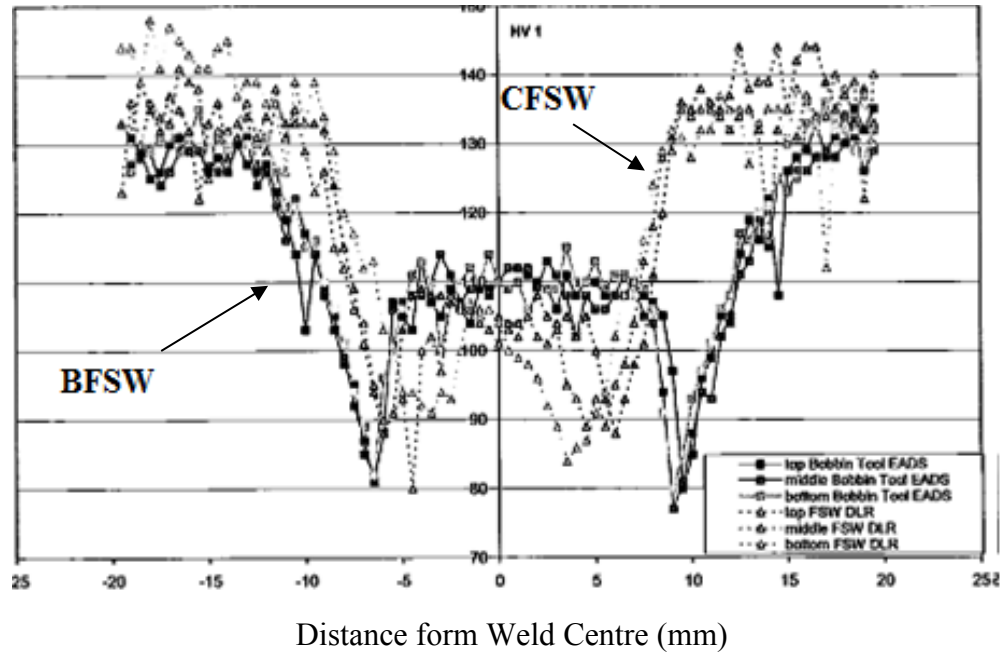
(b)
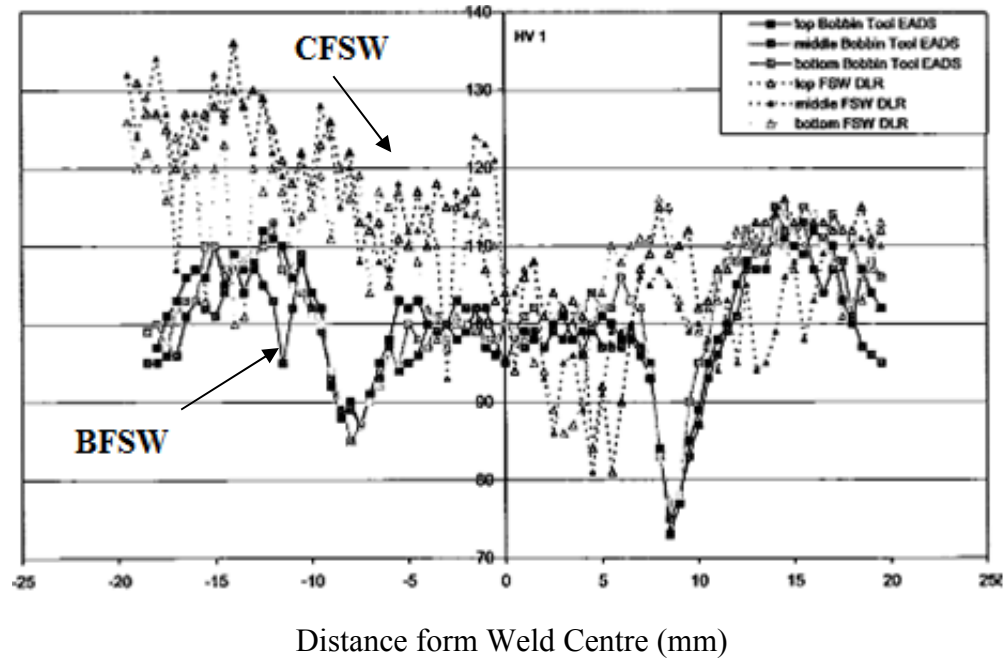
(c)

Figure 2.33: Hardness profile in 6056 Aluminium Alloy as welded condition, (a) T8 (b) T6 (c) T4 [78]

The lowest hardness zones were more confined in BFSW than in CFSW. Moreover, for transverse tensile properties, they found that the bobbin tool specimens exhibited both lower strength (yield stress and ultimate stress) and ductility (elongation) than CFSW

with failure onset being prone at the advancing side. For CFSW the three materials averaged around 300 MPa of ultimate stress, 225 MPa of yield stress and 2% elongation while for the BFSW the averages were around 250 MPa of ultimate stress, 200 MPa of yield stress and 1% elongation. The loss in ultimate stress was between 7% and 20% of the parent material. It has been suggested that these differences are largely due to the fact that the CFSW process involved active cooling on the bottom surface which altered the temperature. In parallel, the stirring action produced a mixture of different grain sizes which eventually helped to harden the material, when compared to BFSW that has a uniform temperature and coarse grain size [25].

Softening was found in the weld nugget zone (Figure 2.33) for both CFSW and BFSW and dependent on the parent material. For example different studies using a solid solution hardened aluminium alloy (i.e.5083 Al-O) showed that softening would not occur in the FSW process because the 5083 Al-O already contained small grains and the FSW process induced a uniform distribution between coarse and fine grains which essentially introduced an increased (better) of hardness profile in the weld [8]. In addition, it is noted that in either CFSW or BFSW the tensile properties of the welded plate was found to be lower than the parent material (but higher than fusion welding) [79][80].

F.F. Wang et al. [81] investigated the effect of rotational speed on micro hardness. They observed two different hardness profiles i.e. U-shaped and W-shaped at mid-thickness, in case of BFSW at constant welding speed of 42 mm/min (Figure 2.34). For low rotational speed e.g. 400 rpm, the hardness drops progressively before reaching a minimum of 85 Hv (59% of the BM) near the edge of the SZ, and rises slightly to a level of 88 Hv within the center SZ. That is, a U-shaped hardness profile is obtained along the cross section. With increasing rotational speeds, e.g., 600–1000 rpm, the hardness rises above 104 Hv within the SZ after reaching a minimum; this indicates that W-shaped hardness profiles are obtained.
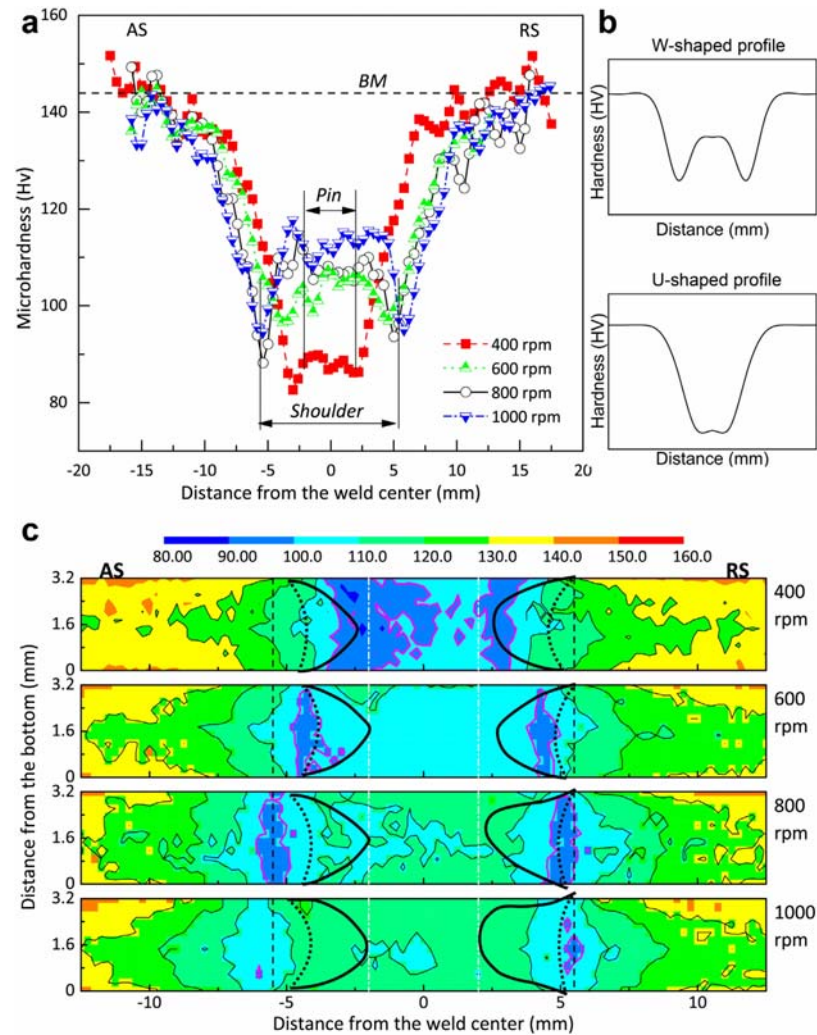
Figure 2.34: (a) Hardness along the mid-thickness of the joints at different rotational speeds; (b) schematic of W-shaped and U-shaped hardness profiles; (c) 2D hardness maps through the joints superposed with the border of TMAZ/SZ (thick solid black lines) and HAZ/TMAZ (dotted black lines). The dashed black lines and dash-dot white lines denote the position of the edge of the shoulder and of the probe, respectively [81].

Postweld heat treatments (PWHT) were introduced by researchers [12] to improve the strength and ductility of the welded plate. A unique observations are presented by M. Ericsson et al. [82]; the T6 material had a proof strength of 130-135 MPa, and a tensile strength of 220 MPa in the friction stir welded condition. The elongation was 7 %. While the T4 + PWAT specimens had a yield strength of 260 MPa, and a tensile strength of 289 MPa. These are higher values than for T6 due to the post weld heat treatment.

Strengthening particles that have been dissolved during the weld thermal cycle are reprecipitated. The elongation was 7 to 8 %.

2.6 DEFECTS AND DEFECT DETECTION IN FSW

The defects like porosity, slag inclusion and solidification cracks are generally associated in fusion welding process which deteriorate the weld quality and joint properties .
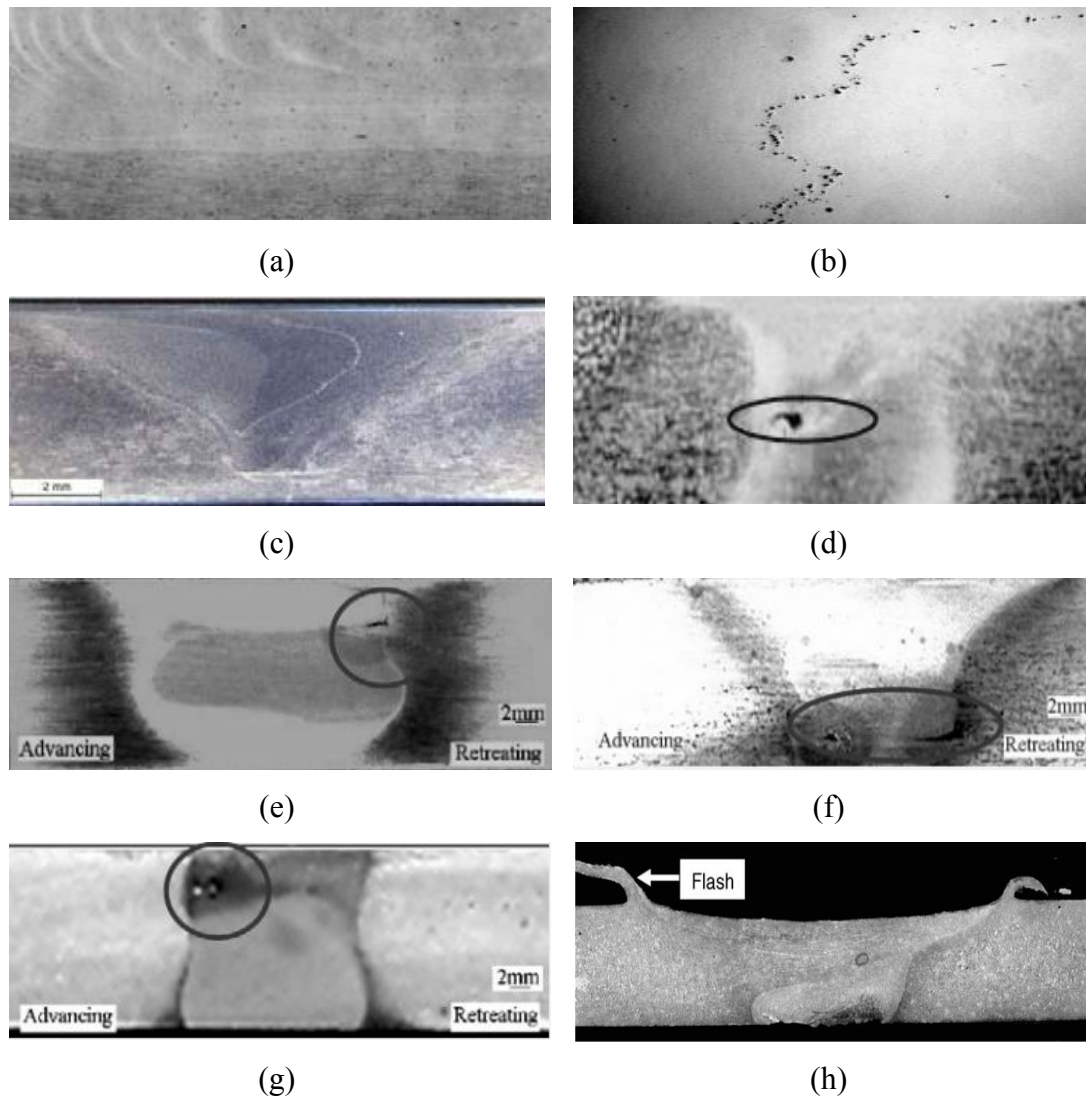

Figure 2.35: Macrostructures identification of defects in FSW (a) incomplete root penetration[12], (b) kissing bond [12], (c) Joint line remnant (JLR) [83] (d) void [58], (e) pin hole [77], (f) worm hole [77], (g) tunnel [77], (h) flash [84].

But in FSW, welded joints are free from solidification related defects because no melting takes place during welding. Despite this, FSW joints are not always free from defects as shown in Figure 2.35. Typical defects are incomplete root penetration and joint line remnant (also termed entrapped oxide defect, piping defect, kissing bond, zig-zag line and lazy S). Defects, that are difficult to avoid, are known as void, unfilled region and volumetric defect (also called pin, worm and tunnel hole) and flash [47][85].

Incomplete root penetrations (refer to Figure 2.35(a)) are the defect found in CFSW. The causes include local variations in the plate thickness, poor alignment of tool relative to the joint interface, and improper tool design. In the realm of tool design (refer to Tool design section), incomplete root penetration occurs when the CFSW pin is too distant from the backing plate. Thus, some of the material at the root is not affected by the stirring flow effect.

When subjected to a bending stress, the friction stir weld will fail along the lack of penetration line. If the pin length is designed equal to the thickness of the plate to be welded, the stirring force causes backing plate contamination in the welded plate. An example of this defect was referred to by Thomas et al. [25] in their studies of welding 12% chromium alloy (as shown in Figure 2.36), with a carbon steel backing plate which contaminated the chromium alloy resulting in a serious impact on localized corrosion resistance.
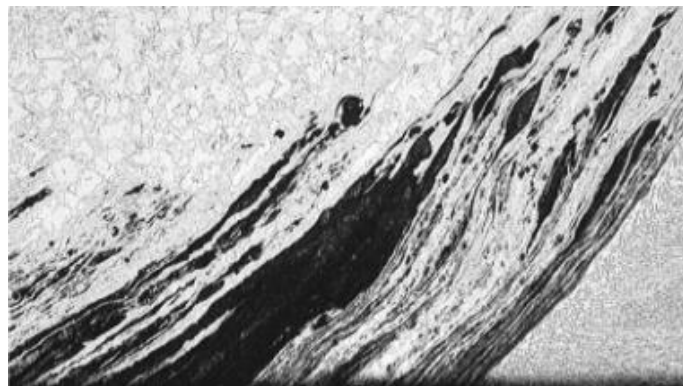

Figure 2.36: Backing plate contamination [25].

Based on Mishra and Ma [12] a joint line remnant (JLR) defect is due to a semi-continuous layer of oxide through the weld nugget (refer to Figure 2.35(b) and Figure 2.35(c)). The semi-continuous layer of oxide was initially a continuous layer of oxide on the faying surfaces of the plates to be joined. The formation of this defect in welding is because of insufficient cleaning of workpieces prior to welding or insufficient deformation at the faying surface interface due to incorrect tool location relative to the joint line, too fast a welding speed, or too large a tool shoulder diameter. Furthermore, by referring to Rajakumar et al. [77] and Sato et al. [86] the kissing bond defect that is grouped under joint line remnant defects is actually a partial remnant of the unwelded butt surface below the stir zone, which is mainly attributed to insufficient plunging of the welding tool during CFSW. The mechanism of the kissing bond is related to insufficient breakup of the oxide layer due to the inadequate material flow of the contacting surfaces around the welding pin. The reason being that is because of the reduction of heat input, which results in insufficient breakup of the oxide layer.

A void formation (Figure 2.35(d)) is due to insufficient forging pressure in the case of CFSW, too high a welding speed, and insufficient workpiece side clamping (too large a joint gap). Material deformed by the friction stir tool must be able to fill the void produced by the traversing pin. If the tool design is incorrect, for example the pin or shoulder diameter is too small for selected welding parameters, the deformed material will cool before the material can fully fill the welding region [3][12][87]. Additionally researchers have identified voids that occur near the top surface of the weld zone, as pin holes, and near to the bottom surface, as worm holes. While a tunnel hole is a long hole defect that runs along the weld, either on the surface or subsurface. These defects are due to the weld material being unable to accommodate the extensive deformation during welding [7][53].

It is found that most of the welding defects listed in this section such as incomplete root penetration, backing plate contamination and void defects, are eliminated or minimized when using BFSW. This is because of high tool friction and no cooling influence introduced by the backing plate in BFSW process. The main issue of BFSW under

idealized condition is not weld defects but the microstructure evolution and obtaining the required welding properties.

2.7 CORROSION

2.7.1 Introduction

Corrosion is defined as the deterioration or destruction of a material by chemical or electro chemical reactions with its environment [88]. Due to corrosion the useful properties of a metal like malleability, ductility, electrical conductivity and also the surface appearance are compromised. The most familiar example of corrosion is the rusting of iron when exposed to atmospheric conditions.

2.7.2 Corrosion of Aluminium

Aluminium is highly reactive, with a negative standard electrode potential of -1660mV, and is therefore unstable in the presence of water. However aluminium reacts quickly with the oxygen in air or water to form a protective oxide film (alumina, Al_2O_3) that is stable in pH range 4-9 and prevents corrosion of the metal.

In aqueous solutions, the oxide film is formed during the reaction:

Oxidation Reaction: $2Al_{(s)} + 3H_2O_{(l)} \rightarrow Al_2O_{3(s)} + 6H^+_{(aq)} + 6e^-$ (2.6)
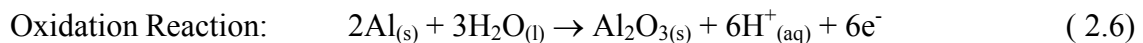
This thickness of the oxide layer can be between 1-10nm, and the speed at which it grows is dependent on temperature and pH [89]. The oxide layer forms within 1 ms in aqueous environments and is protective as it is resistant to dissolution in neutral environments, and blocks the cathodic reaction as it is an insulator.

Although surface oxide layer of aluminium acts as an efficient insulator preventing electron transfer to the surface, commercial alloys contain intermetallic particles that have thinner and more conducting oxide layers allowing electrons to pass through, so that anodic and cathodic reactions can take place [90].
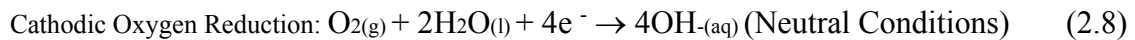
2.7.2.1   Anodic Dissolution

Anodic active dissolution or oxidation is the loss of electrons from an Al atom to leave an Al ion plus electrons. This reaction is given below:

Anodic Dissolution: $\quad\quad Al \rightarrow Al^{3+} + 3e^{-}$ (2.7)

In order for the charge balance to be maintained, the electrons created must be used up in a cathodic reduction reaction.

2.7.2.2   Cathodic Reduction

The main cathodic reactions involve reduction of oxygen or water as shown in the reactions below depending on the environmental conditions:

Cathodic Oxygen Reduction: $O_{2(g)} + 2H_2O_{(l)} + 4e^{-} \rightarrow 4OH^{-}_{(aq)}$ (Neutral Conditions)   (2.8)

Cathodic Water Reduction: $2H_2O_{(l)} + 2e^{-} \rightarrow 2OH^{-}_{(aq)} + H_{2(g)}$ (Neutral Conditions)   (2.9)

Under neutral pH conditions the oxide layer is a good insulator in preventing electrons from reaching the surface preventing dissolution. However at highly acidic and highly alkaline pH values aluminium's passive film becomes unstable and dissolves to leave the bare untreated metal so that active dissolution can take as indicated above in Equation (2.7). Figure 2.37 is a potential v/s pH (Pourbaix) diagram which shows the theoretical regions of immunity, passivity, and corrosion as potential and pH change, whereby lines (a) and (b) indicate the lower and upper limits of corrosion with oxygen reduction, respectively.
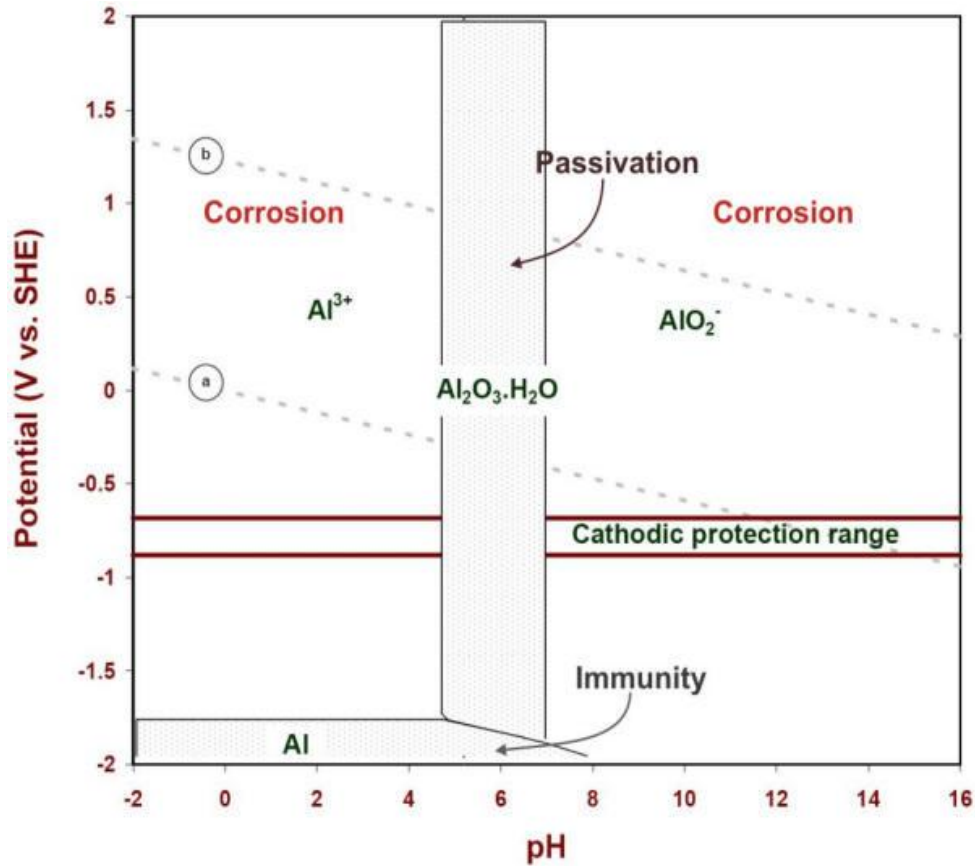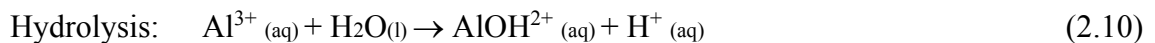
Figure 2.37: E-pH corrosion (Pourbaix) diagram of aluminium in the presence of water at 25°C, showing regions of immunity, passivation and corrosion [90] [91]

The Al^{3+} ions generated at the anode react with water (hydrolysis) to produce local acidity:

Hydrolysis: $Al^{3+}_{(aq)} + H_2O_{(l)} \rightarrow AlOH^{2+}_{(aq)} + H^+_{(aq)}$ (2.10)

Aluminium can also undergo active dissolution in alkaline conditions:

Alkaline Dissolution: $Al_{(s)} + 4OH^-_{(aq)} \rightarrow Al(OH)_4^-_{(aq)} + 3e^-$ (2.11)
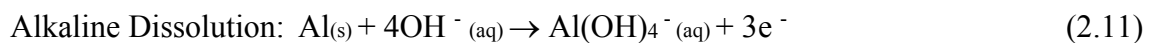
Localized corrosion can take a number of forms however is essentially promoted through the same principle; Firstly the passive film becomes damaged or impaired allowing dissolution to take place. Secondly dissolution products (ions) react with water, creating ions and leading to an increasingly acidic environment. Finally the acidic environment increases the rate at which dissolution takes place because it further prevents the passive oxide layer from reforming, thus corrosion continues to worsen.

55

2.7.3 Corrosion Mechanisms in Aluminium

There are four main types of localized corrosion that affect aluminium in aqueous environments: pitting corrosion, intergranular corrosion, exfoliation corrosion and intragranular corrosion, whereby the mode of corrosion that takes place depends strongly on the alloy, its processing history and its environmental conditions.

Pitting can be a severe form of localized corrosion and is the development of cavities in the surface of the metal. There are two steps in the pitting mechanism, firstly pit initiation, followed by pit propagation. Pitting is often initiated by surface defects or intermetallic particles at the surface and the presence of chlorides which damage the oxide layer [92].
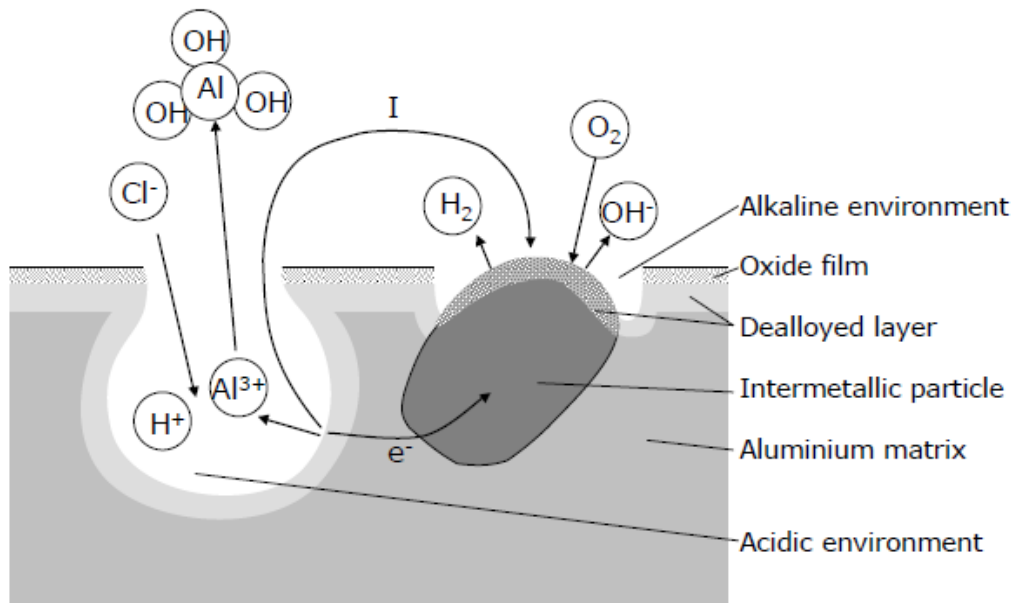

Figure 2.38: Mechanism of pitting corrosion of aluminium alloys [93]

Although barely visible from surface observations, pits can often grow unseen beneath the surface of the metal for some time before blistering. Pit propagation does not occur in all initiated pits; however those that do follow the series of steps illustrated in Figure 2.38 [93] which can lead to severe pitting as shown in Figure 2.39 [94] and 2.40 [95].

- The damaged oxide layer leads to anodic dissolution of Al at the base of the pit, where electrons are transported to the surface and used in cathodic reactions.

56

- Al^{3+} ions are used in hydrolysis reactions leading to acidification within the pit, preventing formation of an oxide film within the pit.

- Chloride ions (Cl^-) are drawn into the pit to balance the positive charge generated by anodic reactions, producing a more aggressive environment preventing repassivation of the oxide layer so Al dissolution continues.
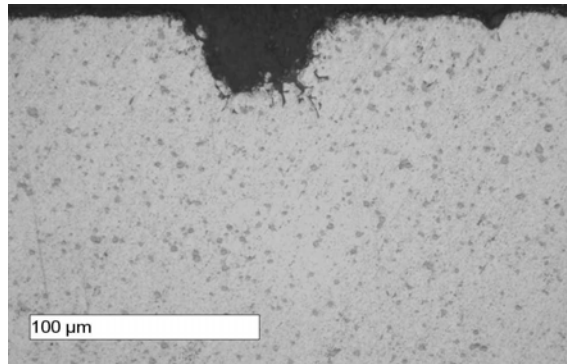

Figure 2.39: Cross section of pitting attack on AA6082 aluminium alloy after exposure to marine atmosphere for 6 months. The dark spots are intermetallic particles [94]
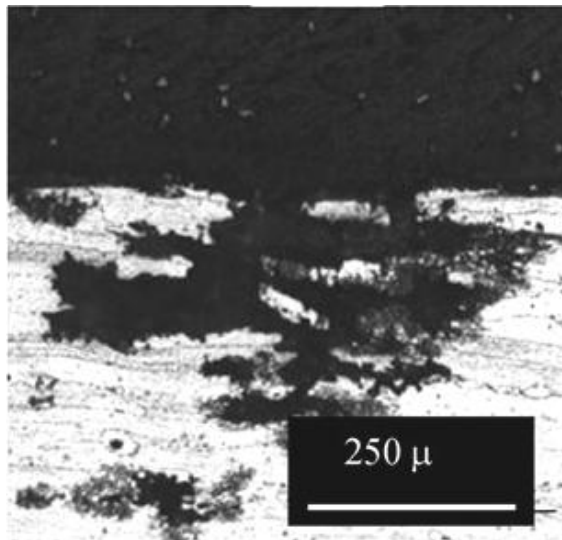
Figure 2.40: An example of severe pitting attack in HAZ of FSW AA7075-T651, with attack at the precipitate-free zone following immersion testing in 3.5 wt.% NaCl solution [95]

Intergranular corrosion (IGC), as shown in Figure 2.41 as a schematic diagram, is attack along grain boundaries or closely adjacent regions, without attack of the grain interior, and is caused by a difference in corrosion potential between grain boundary region and the grain itself. IGC can be caused by precipitation of anodically active

intermetallic particles on the grain boundaries, which corrode preferentially. It can also be caused by precipitation of more noble precipitates, particularly those containing copper, since this leads to formation of a copper depleted region adjacent to the boundary, which is more susceptible to anodic dissolution than the copper-rich matrix in the grains. Figure 2.42 [95] illustrates the presence of a Cu depleted zone surrounding Cu rich precipitates that form along a grain boundary. The Cu depleted zone has a lower corrosion potential compared with the surrounding Al matrix and the Cu rich precipitates at the grain boundary and so goes into dissolution preferentially via microgalvanic coupling [96].

Figure 2.41: Schematic diagram showing the role of the copper depleted zone in IGC

IGC can lead to intergranular stress corrosion cracking (IGSCC), which is the simultaneous interaction of sustained tensile stress and corrosion processes, leading to crack initiation and propagation which can result in premature brittle failure of a ductile material.
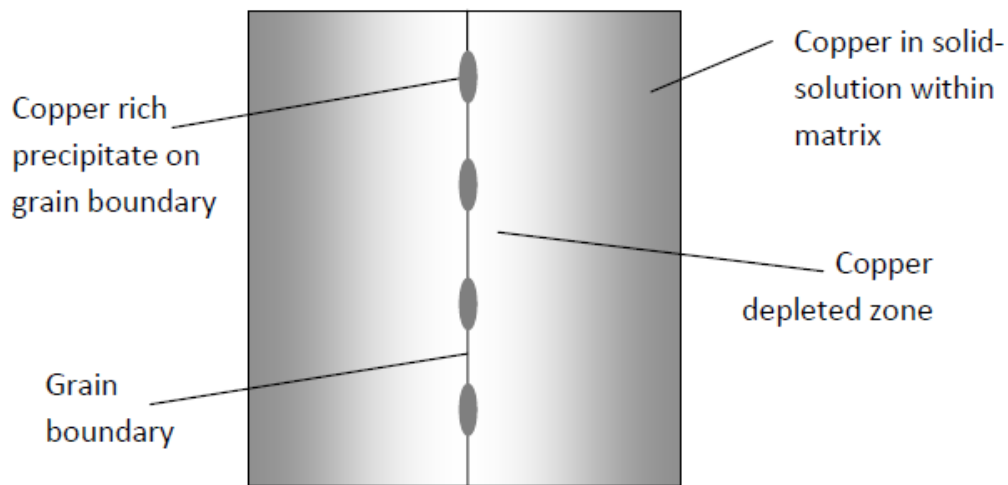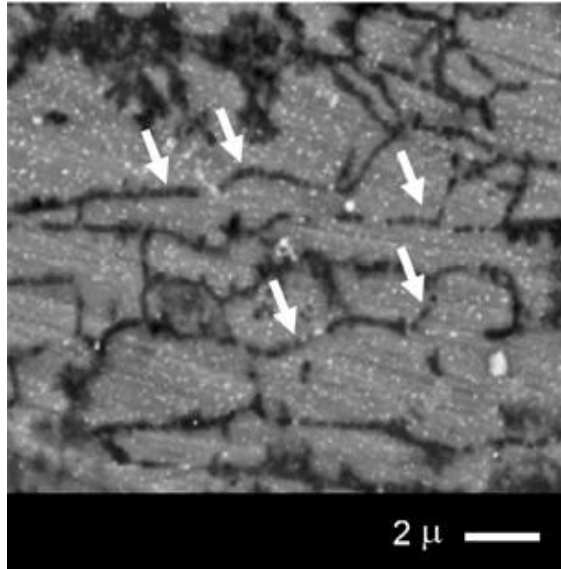
Figure 2.42: Initial stages of IGC in the HAZ of FSW AA7075-T651, with attack at the precipitate-free zone: Note the presence of small "white" grain boundary precipitates (arrows) and attack of the precipitate-free zones (black) [95]

Intragranular corrosion, sometimes considered as technically a form of pitting, is when the grain interior corrodes preferentially to the grain boundary. Often a result initially of pitting at the surface, followed by intergranular corrosion through the material following grain boundaries, until a grain is reached that will corrode preferentially to the grain boundary. Intragranular susceptible grains are often those with a higher than average dislocation density, leading to either a high degree of precipitation of active precipitates, or a reduction of copper in solid solution through copper rich phases forming at sub-grain boundaries.

Exfoliation corrosion, as shown in Figure 2.43 is another form of localised corrosion that propagates along planes parallel to the rolling direction [97]. It is often as a consequence of IGC whereby the voluminous corrosion products are unable to dissolve into the environment and instead form along the paths of attack causing internal stresses leading to layers of metal being lifted from the surface [98]. It is a process that more often occurs in metal with strong directionality which creates highly elongated grains.
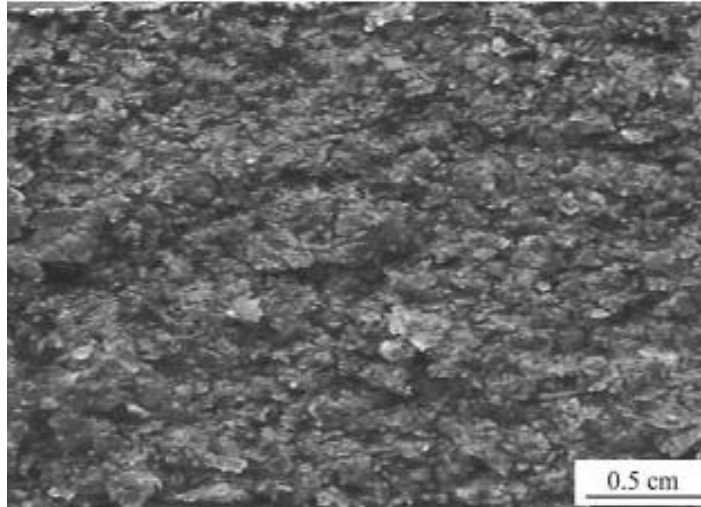
Figure 2.43 : An example of exfoliation corrosion on the surface of an Al-Li alloy following an immersion test of 96h in EXCO solution [97]

2.7.4   Influence of alloying elements

High purity aluminum is very corrosion resistant because of its surface oxide layer. But, its strength is insufficient for most practical applications [89], so it is required to be alloyed with elements such as Cu, Mg, Li, Zn, Mn, Si.

The corrosion resistance is badly affected because of additional alloying [99]. When the alloying elements are in solid solution the alloy generally remains corrosion resistant, however corrosion resistance or alloys is reduced due to precipitation and the formation of second phase particles. These second phase intermetallic particles can form during solidification either through cellular/dendrite boundaries, and can be anodic, inert, or cathodic to aluminium [92]. Those particles that are more electrochemically active than aluminium act as localized anodes and go into dissolution themselves, while those that are less electrochemically active become net cathodes relative to the aluminium matrix where dissolution will occur.

2.7.5   Corrosion of Friction Stir Welded Aluminium Alloys

Generally, it has been found that the weld zones are more susceptible to corrosion than the parent metal. Friction stir (FS) welds of aluminium alloys such as 2219, 2195, 2024, 7075 and 6013 did not exhibit enhanced corrosion of the weld zones [100]. FS welds of

aluminium alloys exhibit intergranular corrosion mainly located along the nugget's heat-affected zone (HAZ) and enhanced by the coarsening of the grain boundary precipitates.

The effect of FSW parameters on corrosion behaviour of friction stir welded joints was reported by many researchers [101][102]. The investigations by Surekha et al. [102], on the high strength precipitation hardenable alloy AA2219-T87; indicate that tool rotation speed influences the rate of corrosion. Which is attributed to the breaking down and dissolution of the intermetallic particles. Jariyaboon et al. [101] studied the effect of welding parameters (rotation speed and travel speed) on the corrosion behaviour of friction stir welds in the high strength aluminium alloy AA2024–T351. They also found the similar result of rotational speed having about the location of corrosion attack. Localized intergranular attack was observed in the nugget region for low rotation speed welds, whereas for higher rotation speed welds, attack occurred predominantly in the HAZ.

Many investigators studied the corrosion resistance of Al alloys weld joints made by using FSW and other conventional fusion welding techniques such as Metal Inert Gas (MIG) and Tungsten Inert Gas (TIG) [103][104]. For instance, a comparison of the corrosion resistance of AA6060T5 and AA6082T6 joints made by Friction Stir Welding (FSW) and Metal Inert Gas (MIG), respectively, is reported by Stefano and Chiara [104]. Tests were conducted by putting the welded and polished samples in an acid salt solution. Corrosion resistance was detected via morphological analysis of the surface. The attack was localized (pitting), an index referred to the pit density was used for the comparison. The results indicated that joints welded using FSW are more resistant to corrosion than those welded using MIG. An experimental investigation has been carried out, by Squillace et al. [103], on microstructure and corrosion resistance of weld butt joints of AA 2024-T3 welded using FSW and TIG techniques. Polarization curve tests and electrochemical impedance spectroscopy showed a nobler behaviour of weld bead with respect to parent alloy. In FSW joints, however, the differences between the nugget, thermo-mechanically affected zones (TMAZ) and heat affected zones (HAZ) were not so evident as in TIG joints; what is more, inside FSW weld bead, the retreating zone showed a behaviour nobler than the advancing one.

Muna K. Abbass et al. [105] studied the effect of heat treatment on the corrosion resistance of friction stir welded AA2024 aluminum alloy using 3.5%NaCl solution at a

temperature of 30ºC. After performing age or precipitation heat treatment for welded joint at 510ºC and aging at 190ºC, it was noticed that corrosion current (Icorr) is lower than that of base alloy and improve the corrosion resistance of weld because of precipitation homogeneity occurring in the microstructures of various welding regions. It is shown that the corrosion behavior of base alloy significantly varies from that of welded joints, and the friction stir welds have higher corrosion rates than base alloy. This is due to inhomogeneity of microstructure in weld regions.

The other researcher Litwinski [106], found that, the weld travel speed/cooling rate has an appreciable effect on the weld corrosion resistance. While Gharavi et al. [107] had a different outcome in case of lap welds by FSW. The parent alloy of 6061-T6 is found to be more susceptible to pitting and intergranular corrosion. The corrosion resistance in the top half of the WNZ for lap joint is better than that of bottom half.

The corrosion resistance of the stirred zone, at the center of the welded zones, was found to be reduced by increase of tool rotational speed and/or reduction of the welding speed in case of cast alloys A319 and A356 [108]. Both the upper regions of the squeezed zone and the adjacent thermo-mechanically affected zone have corroded very severely [108].

At the current stage, corrosion resistance between the CFSW and the BFSW could not be differentiated due to limited sources of available literature in BFSW but both are threatened by potential inferior corrosion characteristics. Example studies for CFSW are shown in Figure 2.44 [109] for corrosion attack of 7075Al-T651 following exposure to a 4M NaCl-0.5M KNO_3 -0.1 M HNO_3 environment. It was evident that after 24 hours exposure (Figure 2.44 (a)) to the solution, the corrosion was much localized in the HAZ, including the outer edges of the TMAZ, and neither the base alloy nor the weld nugget showed evidence of corrosive attack. For extended exposure hours, the intergranular attack became more severe in the initial attack region and the attack region spread to the entire TMAZ regions previously unattacked (Figure 2.44 (b)). Finally, the intergranular attack was also developed in the nugget zone. However, no intergranular corrosion was detected in the parent metal (Figure2.44 (c)).
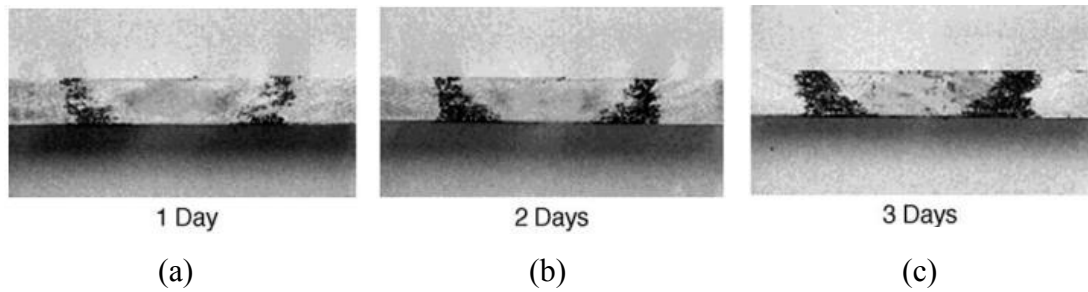
Figure 2.44: Corrosion attack on CFSW of 7075Al-T651 Al [109]
(a) 1 day. (b) 2 days (c) 3 days.

For the BFSW process an example of corrosion behaviour can be found in Allehaux and Marie studies [110] when they welded 2139 Aluminium-Copper Alloy. The corrosion test was in accordance with ASTM G110 whereby the specimen was immersed in an aqueous attack solution of $NaCl+H_2 O_2$. The test was performed on as welded plate (without aging) and as welded with aging (post weld aging). The conclusions from their studies were as welded plate (without aging) and the advancing side of both types of welded plate (as welded and as welded with aging) have better resistance to corrosion attack.

It can be stated that based on this literature survey generally CFSW joints have better weld properties compared to BFSW but the advantages in BFSW which were stated in the Introduction section still indicate high levels of promise for the process. Furthermore, it is evident that further studies are required in order to reveal the true potential of the BFSW process.

2.8   INFRARED THERMOGRAPHY

2.8.1   Introduction

The process of generating visual images representing variations in IR radiance of objects is known as Infrared (IR) thermography. Objects of different materials and colors absorb and reflect electromagnetic radiation in the visible spectrum of light (0.4 to 0.7 microns) similarly at temperatures above absolute zero (-273 $^{\circ}$C), every object emits IR energy proportional to its existing temperature. The IR radiation spectrum do exist between 2.0 to 15 microns. A 2D visual image reflective of IR radiance from object surface can be

generated by IR sensitive electromagnetic radiation detector. The process is similar to that as video camera uses to detect a scene reflecting electromagnetic energy in the visible light spectrum. The information captured is interpreted, and displayed, what it detects on a liquid crystal display (LCD) screen that can then be viewed by the device operator [111].
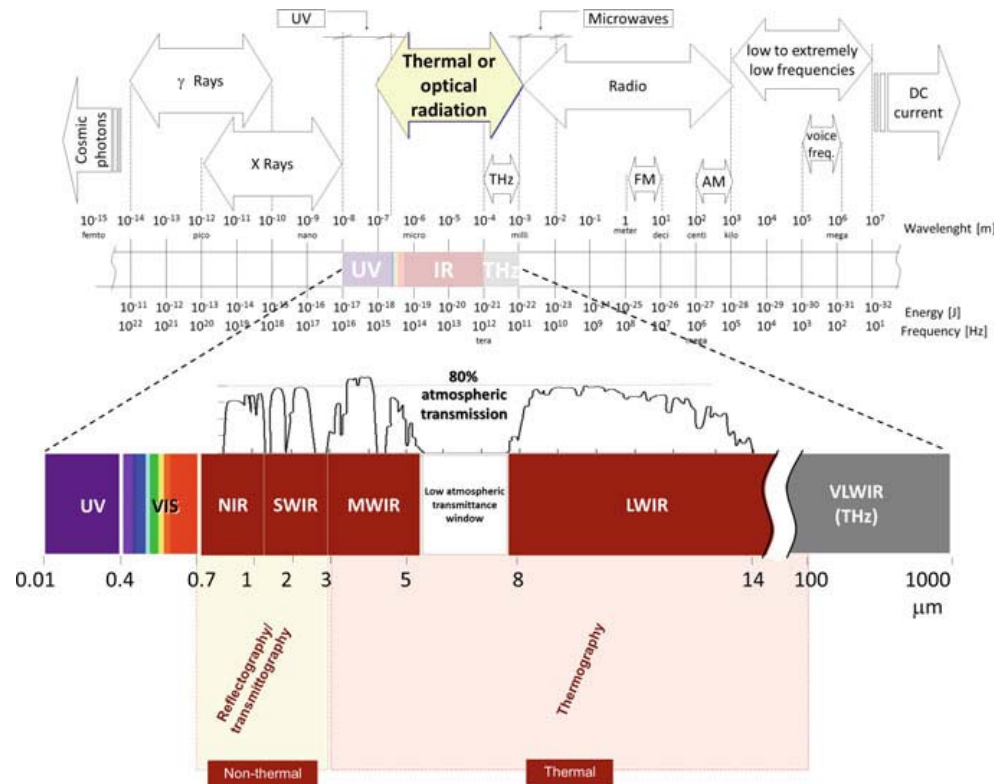

Figure 2.45: The infrared bands in the electromagnetic spectrum [112]

IR radiation is invisible to naked eyes as it falls outside that of visible light (the radiation spectrum to which our eyes are sensitive). An IR camera or similar device allows to view an object (based on its temperature and its proportional emittance of IR radiation) beyond visible spectrum of light. Figure 2.45 shows classifications based on the atmosphere high-transmission windows as well as the type of detector materials that are sensible on each particular band. Four IR spectral bands are of interest for infrared vision applications: (1) the near infrared (NIR, from ~ 0.7 to 1 µm), (2) the short-wave IR (SWIR, from ~1 to 2.5

μm), (3) the mid-wave infrared (MWIR, from ~ 3 to 5 μm), and (4) the long-wave infrared (LWIR, from ~ 7.5 to 14 μm) [112].

A formal definition has been proposed as: "Infrared thermography is a nondestructive, nonintrusive, noncontact technique that allows the mapping of thermal patterns, i.e., thermograms, on the surface of objects, bodies or systems through the use of an infrared imaging instrument, such as an infrared camera" [113].

2.8.2   Brief History of Thermography

As with most technologies, thermal imaging systems are based on phenomena discovered nearly 200 years ago [114][115]. Sir William Herschel discovered infrared rays (light) on February 11, 1800. He studied the spectrum of sunlight with a prism [116] (Figure 2.46), measuring temperature of each colour.
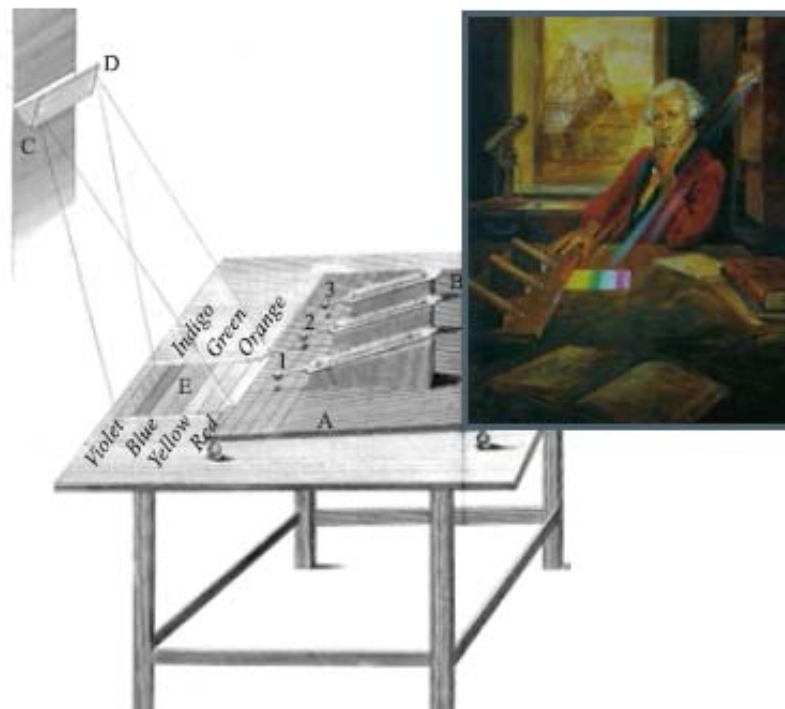

Figure 2.46: Herschel's first experiment: A,B – the small stand, 1,2,3 – the thermometers upon it, C,D – the prism at the window, E – the spectrum thrown upon the table, so as to bring the last quarter of an inch of the red colour upon the stand. Inside Sir Frederick William Herschel (1738–1822) measures infrared light from the sun [116]

Later, John Herschel (1840) produced the first infrared image using a method that he called evaporography. By evaporating alcohol from a carbon-coated surface, a visible image was produced. This was the first thermogram. It took another 89 years (1929) before Czemy provided an improvement to image creation.

In the case of thermography, some of the advantages and limitations with respect to other NDT methods are as follows [113].

2.8.3 Advantages

- Fast inspection rate;
- Contactless, IR imager is kept away from the object or specimen to be tested. Coupling media between the transducer and the specimen as in Ultrasonic Test is not required.
- Security of personnel, there is no harmful radiation involved as in the case of x-ray radiography.
- IR images are obtained in the form of Images or video, they are easily interpreted and results are obtained.
- There are number of applications;
- It very easy to learn or train the personnel as compare to ultrasonic or X-ray operations.

2.8.4 Limitations

- The IR thermographic camera and thermal simulation units are costly.
- Capability to detect only defects resulting in a measurable change of the thermal properties from the inspected surface;
- Thermal losses by convection and heat radiation that might induce spurious contrasts
- Affecting the reliability of the interpretation;
- Ability to inspect a limited thickness of material under the surface,

- Emissivity variations, low emissivity materials strongly reflect thermal radiations from the environment, the results may be erratic. Surface painting can be employed to increase and equalize emissions when possible.

Majority of the researchers have adapted IR thermography for NDE, tensile test, fatigue test and predictive maintenance purpose [119] [120][121][122]. Marina M. Kutin et al. [119] studied the tensile test with continuous non-contact thermography and observed that, this technology enables conducting stress analysis and estimation of plastic deformation limits within a shorter period than in other nondestructive and non-contact method. During the tensile test, the thermography gives visible data of temperature changes on the surface of specimen. This proves that the variations in temperature captured by the IR camera are strongly correlated to the loads actually applied to the specimen.

Transient - active thermography has emerged in recent years as a means of NDT & E technique. Its advantages are that it is a rapid large area non-contact imaging technique that produces images of subsurface features (i.e. defects) that are relatively straightforward to interpret [123].

Esther T. Akinlabi et al. [124] presented an idea of using IR camera for FSW. They stated that, it is not possible to obtain actual experimental data and Thermographic images without conducting an actual FSW procedure with the thermographic monitoring. A simulation of the expected result is depicted in Figure 2.47.

Note that the color scale shown on Figure 2.47 does not depict actual temperature variations during a FSW process. These values are assumed and only serve to present an example of the expected visual results of the temperature monitoring system.

The detailed performance analysis and simulation showed that the concept of employing an Infrared Thermography will be suitable for the temperature monitoring system of Friction Stir Welding.
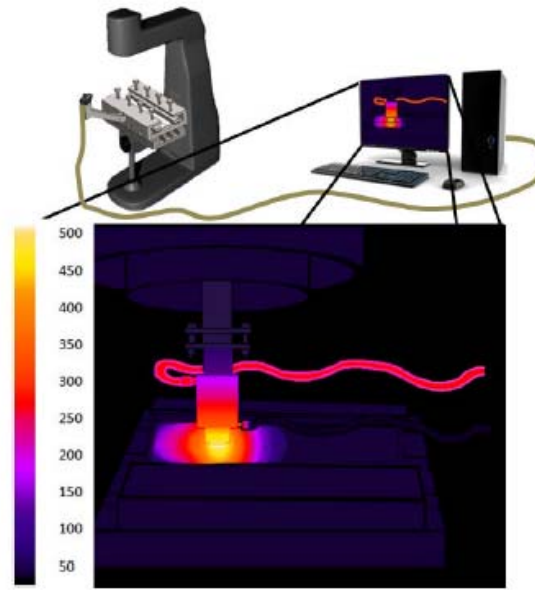
Figure 2.47: Simulated thermographic image during FSW [124]

A FSW and laser assisted FSW bead on plate test was carried out by C. Casavola et al. [125] to study the effect of laser preheating in FSW of AA 5754 H111 alloy using IR thermography.

Figure 2.48: Thermal field at FSW, seen on the infrared image [126]

The experiments have shown that in order to achieve quality welds with a well consolidated nugget covering the entire thickness of the welded materials it is necessary to obtain the optimum plasticizing temperature for these materials. Achieving and

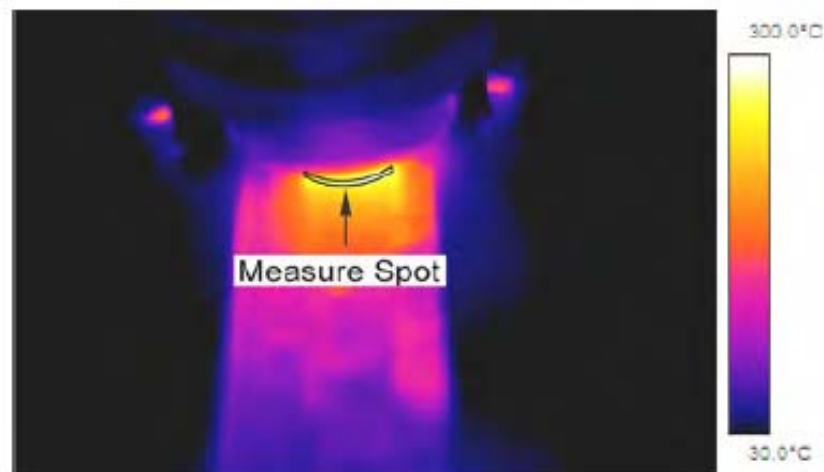maintaining its plasticizing temperature at the optimum level can be tracked on-line (Figure 2.48) on trend charts obtained by using infrared thermography system.

Figure 2.49, presents the FSW temperature evolution of Cu99 plates with a thickness of 5mm. Control of welded joints showed that the optimum temperature at which the welding material must reach in the action zone of the welding tool should be about 640-660 0C, in order to achieve flawless joints, in the case of Cu99 [126].

The presented results in the international symposium contain only a qualitative analysis of possibility of application of the thermal imaging camera for monitoring the Friction Stir Welding processes. The author states that, the presented method is a new method for monitoring the friction stir welding processes using thermal imaging. The obtained results indicate its potential practical application and the method is to be further developed to become a part of a hybrid system for monitoring the FSW processes [127].
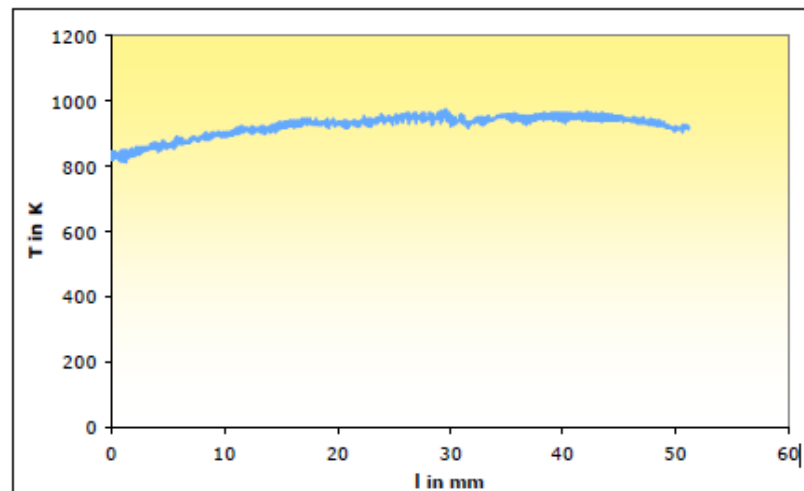
Figure 2.49: Temperature chart for Cu 99, 5mm thickness [126]

Valery E. Rubtsov et al. [128] studied the passive infrared inspection during FSW to analyze the temperature anomalies. They suggested that infrared inspection can be successfully applied for detecting dangerous internal defects directly in the process of welding. However, the comparison of destructive and thermography testing data cannot be interpreted unambiguously in all cases and give adequate information about a detected

internal defect represented on the thermogram; an improved data processing technique need to be adapted to obtain more reliable results.

The infrared camera should be placed normal to the weld direction, in front of the FSW machine suggested by C. Casavola et al. [125]. The optical axis of the camera has been placed with an angle of 60° with respect the horizontal direction. To reduce the reflection of the aluminum and increase the emissivity of the surface, the specimen be painted with matte black acrylic spray paint. An emissivity of $\epsilon = 0.95$ has been set on the camera.

2.9 SUMMARY OF THE STATE OF THE BODY OF KNOWLEDGE

2.9.1 Summary

The author's analysis of the literature is that the factors that affect joint quality are; joint geometry, tool dimensions, pin and shoulder features, rotational directions, welding passes, dwell time, cooling/pre-heating, material microstructure, welding environment, material properties/composition, contamination and support. These additional factors have been drawn from the insight of other published work in the field [7][8][11][13][24][25][29][33][42][50][58][68][71][129][130] and also from the background work done by the author to provide a near comprehensive list, see Figure 2.50. However, the main studies by previous researchers mostly involve tool design, spindle speed and travel speed.

The definition of factors in the cause and effect diagram is as explained below:

Joint type: This is the joint configuration like butt, lap, corner etc. It is important for fixture and tool design.

Fixture design: It includes fixture material, clamp geometry, clamping system, clamping force and heat transfer. The material of fixture is very important from heat conduction point of view.

Tool Design: It includes tool material, pin and shoulder shape, features and dimensions. Also the method of welding (CFSW or BFSW) is considered while designing the tool.

Joint Type   Fixture Design   Tool Design

Butt → Corner   Clamping force ← Material   Tool Material   Pin feature / Pin shape
Lap → Edge   Heat Conduction → Clamp Geometry   Dimensions   Shoulder shape / Shoulder feature
Tee →   Rigidity of clamp system → Position/Location   CFSW BFSW →

Weld Quality

Composition → Properties   Rotational Speed → Rotation direction   Humidity →
Melting point → Microstructure   Travel speed → Tilt angle
Thickness → Oxidation/contamination   Plunge force → Dwell time   Surrounding Temperature

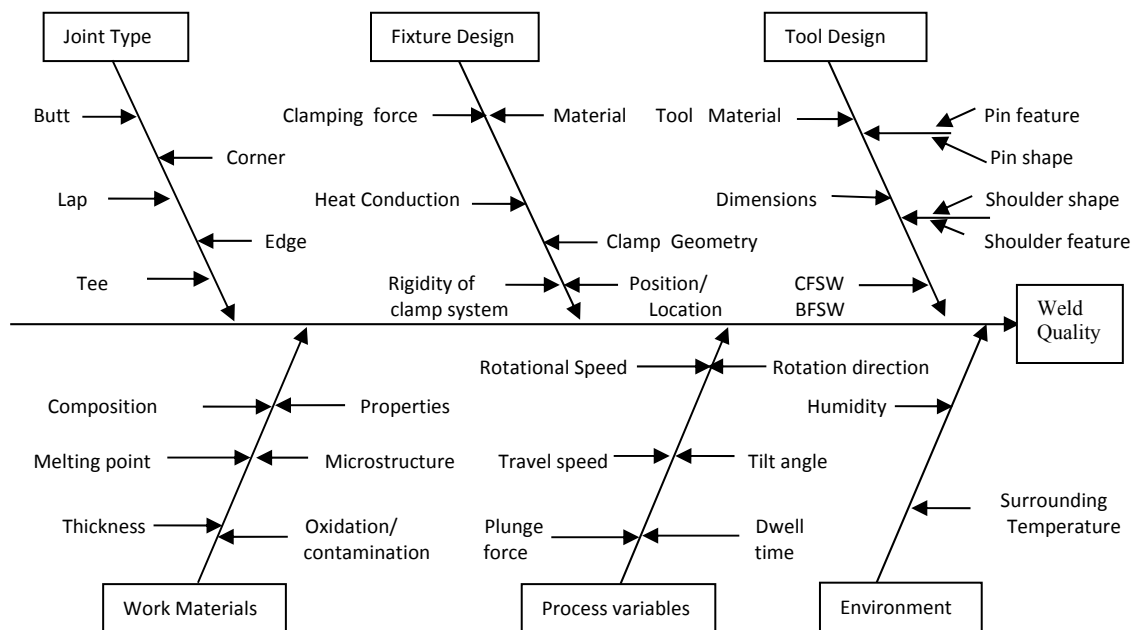Work Materials   Process variables   Environment

Figure 2.50: Cause and effect diagram for proposed work

Pin and Shoulder: The author categorizes these features as the primary features. Each primary feature can be associated with secondary features. For example surface features and shape (refer Tool Design section). In the case of bobbin tool, the additional shoulder at the bottom required the gap to be appropriately set. This is because it will affect tool load hence influence the amount of heat and material flow.

Tool dimension: The dimensions of the tool features such as pin length, pin diameter and shoulder diameter. D/d ratio is used to indicate the relationship between shoulder diameter (D) and pin diameter (d).

Conventional v/s Bobbin tool FSW: The method used will define the fixture and tool design.

Work Material: This is a universal factor. Each material has its own properties and to obtain good weld the material characteristics such as hardness, melting point, wear resistance, thermal coefficient and rigidity are important.

Melting point: Tool properties should be capable of hold up under the generated temperature while stirring the material.

Material composition, microstructure and properties: Different materials will have different resistance to friction which required appropriate welding setting.

Material thickness: This parameter is important in identifying appropriate tool design features and dimensions. More heat is required for thicker materials. In addition, the FSW tool should be capable of withstanding the torque developed while stirring the material.

Oxidation/Contamination: Some of the oxidation/contamination can be displaced from the friction heat generated by the shoulders and some will be trapped inside the weld area. This causes impurity of the weld area or void formation due to the trapped gases.

Process variables: this includes tool rotational speed and direction, tool plunge, dwell time, tool tilting and traversing speed.

Rotational speed: Is the rotational frequency of the spindle of the machine. Also known as spindle speed, measured in revolution per minute (rpm).

Rotation direction: This is the direction of spindle movement. It can be either clockwise or counter clockwise which also interacts with the handedness of tool features.

Traverse speed: Also known as travel speed. The speed of the tool movement on the path of the welding direction, normally measured in millimeter per minute (mm/min) or inch per minute (ipm).

Plunge force: The force that causes CFSW tools to compress into the welding plate. In case of BFSW compression between the shoulders plays this role.

Dwell time: The time taken for frictional heating to build up under the tool prior to a welding run being initiated at the required travel speed for material readiness.

Humidity: The dampness of the air quality while the welding was performed may affect the oxidation.

Surrounding temperature: Plate will be preheated if surrounding temperature is high and extra heat generation will be required if the process is done during cold conditions.

2.9.2   Gaps in the body of knowledge

It is observed from the literature that tool design is the key to the successful application of FSW [42]. The reasons being that are the inherent effects on heat generation and mixing formation of the weld. However at present there is no universal tool for FSW and each tool requires welding process optimization due to the interdependency of each welding feature. Consequently, many studies have been under taken on heat generation and material flow when different tool features and welding parameters were used in order

to understand the thermal and flow effects and so that welding guidelines can be suggested [28][52][130][131]. Besides this there are also researchers who have adopted the design of experiments technique to help optimizing the welding process [27]. However all these studies were done in a piecemeal manner, and primarily for CFSW rather than BFSW. As stated in the beginning of the section, the differences between CFSW and BFSW may seem small, but the additional shoulder has a major effect on the functional consequences.

Clamping of substrate though is most important element in FSW is not given much weightage in designing the clamping system.

The BFSW process is difficult to commercialize because of the process variability, the covert variables, and the unknown relationships of cause and effect. There is a need to optimize the BFSW process for a fixed bobbin tool. However, before the optimization process through modeling or empirical studies can be done, there is a need to identify the process variables and their interactions.

Corrosion studies have not considered much in the research, though it is important in deciding the weld quality and product life.

From the literature it is observed that there is a wide scope and lot of potential in the field of IR Thermogrphy. The research carried out is qualitative and very lean in published literature specifically in case of FSW.

Infrared Thermography (IRT) as a new tool needs to be introduced for online monitoring of weld quality both for CFSW and BFSW. The IR thermography applications in FSW are very less found in the published literature. There is a wide scope and potential in exploring the idea of IRT applied to FSW investigations on quality of weld and defects.